



Published in final edited form as:

Biol Cybern. 2010 January ; 102(1): 9–29. doi:10.1007/s00422-009-0347-0.

Phase-linking and the perceived motion during off-vertical axis rotation

Jan E. Holly,

Department of Mathematics, Colby College, 5845 Mayflower Hill, Waterville, ME 04901, USA
jeholly@colby.edu

Scott J. Wood, and

Universities Space Research Association, Houston, TX, USA

Gin McCollum

Neuro-Otology Department, Legacy Research Center, Portland, OR, USA

Abstract

Human off-vertical axis rotation (OVAR) in the dark typically produces perceived motion about a cone, the amplitude of which changes as a function of frequency. This perception is commonly attributed to the fact that both the OVAR and the conical motion have a gravity vector that rotates about the subject. Little-known, however, is that this rotating-gravity explanation for perceived conical motion is inconsistent with basic observations about self-motion perception: (a) that the perceived vertical moves toward alignment with the gravito-inertial acceleration (GIA) and (b) that perceived translation arises from perceived linear acceleration, as derived from the portion of the GIA not associated with gravity. Mathematically proved in this article is the fact that during OVAR these properties imply mismatched phase of perceived tilt and translation, in contrast to the common perception of matched phases which correspond to conical motion with pivot at the bottom. This result demonstrates that an additional perceptual rule is required to explain perception in OVAR. This study investigates, both analytically and computationally, the phase relationship between tilt and translation at different stimulus rates—slow (45°/s) and fast (180°/s), and the three-dimensional shape of predicted perceived motion, under different sets of hypotheses about self-motion perception. We propose that for human motion perception, there is a phase-linking of tilt and translation movements to construct a perception of one's overall motion path. Alternative hypotheses to achieve the phase match were tested with three-dimensional computational models, comparing the output with published experimental reports. The best fit with experimental data was the hypothesis that the phase of perceived translation was linked to perceived tilt, while the perceived tilt was determined by the GIA. This hypothesis successfully predicted the bottom-pivot cone commonly reported and a reduced sense of tilt during fast OVAR. Similar considerations apply to the hilltop illusion often reported during horizontal linear oscillation. Known response properties of central neurons are consistent with this ability to phase-link translation with tilt. In addition, the competing “standard” model was mathematically proved to be unable to predict the bottom-pivot cone regardless of the values used for parameters in the model.

Keywords

OVAR; Model; Vestibular; Perception

1 Introduction

Non-veridical perceptions of self-motion often arise during passive whole-body motion without vision, such as in a vehicle or experimental apparatus. While certain non-veridical perceptions are easily explained by well-understood principles, other perceptions still evade scientific explanation, especially when the perception does not match the motion predicted by eye movements. For complex motions, especially, there is increasing evidence that the perceived motion may not be the motion for which the eye movements are apparently compensating through gaze stabilizing mechanisms. This perception-eye mismatch has been found, for example, in centrifuges (Guedry et al. 1992; McGrath et al. 1995; Mittelstaedt and Jensen 1999), tilt and translation motions (Merfeld et al. 2005a,b; Zupan and Merfeld 2005), and off-vertical axis rotation (Wood et al. 2007). The question arises whether perception, as opposed to eye movements, can be understood for complex motions, and whether special principles apply to perception.

Off-vertical axis rotation (OVAR) is a particularly intriguing puzzle. Eye movements and many components of perception have been shown consistent with physical law and time constants. For example, the semicircular canals of the inner ear receive the stimulus of angular acceleration, α , in three dimensions, and the afferent response decays with a time constant on the order of 5–10 s (Fernández and Goldberg 1971). Additional neural processing, most likely through feedback loops, extends the time constant, τ_a , for perceived angular velocity, ω , to closer to 20 s (Guedry et al. 1971). The main dynamics are captured by the first-order equation

$$\frac{d\omega}{dt} = \alpha - \frac{\omega}{\tau_a} \quad (1)$$

which explains the decay of perceived angular velocity during continued rotation. This type of dynamics (reviewed in Guedry 1974; Mayne 1974; Young 1984) is sometimes called “velocity storage.”

However, the full three-dimensional perception during OVAR is nevertheless not predicted by most current models. In OVAR, subjects in the dark are rotated about a diagonal, or tilted, axis (Fig. 1a). The tilt of the rotation axis determines the magnitude of the linear stimulus along the primary response plane of the utricles of the inner ear (Curthoys 1996), which detect linear acceleration stimuli. This tilt can range from a few degrees off-vertical to rotation about an Earth-horizontal axis (referred to as barbecue-spit rotation, e.g., Correia and Guedry 1966). In a typical experiment, the subject is tilted so that the body axis is aligned with the rotation axis, and after start-up effects have subsided, the perceived motion is of progression around a cone or cylinder (Fig. 1b, c) (Denise et al. 1988; Guedry 1974; Vingerhoets et al. 2006; Wood et al. 2007). Although variations other than the bottom-pivot cone or cylinder have been reported (Denise et al. 1988), the bottom-pivot cone is the most common. The cone and cylinder are often explained by appealing to two basic principles of self-motion perception, both of which involve the gravito-inertial acceleration vector (GIA), \mathbf{A} , i.e., the sum of the actual linear acceleration, \mathbf{a}_A , and the upward “pseudo-acceleration”, \mathbf{g}_A , due to the presence of gravity:

$$\mathbf{A} = \mathbf{a}_A + \mathbf{g}_A$$

The physiological system cannot distinguish between \mathbf{a}_A and \mathbf{g}_A , so \mathbf{A} is the stimulus to the otolith organs of the inner ear (reviewed in Goldberg and Fernández 1984) and somatic graviceptors (Mittelstaedt and Mittelstaedt 1996). The two principles that are typically used to explain the conical perception during OVAR are based upon well-known properties of perception (Guedry 1974; Mayne 1974) and are as follows: (1) over time, the perceptual system

tends to use \mathbf{A} as the indicator of vertical, which causes the subject's internal estimate, \mathbf{g} , of \mathbf{g}_A to progressively tilt toward \mathbf{A} :

$$\frac{d\theta}{dt} = -\frac{\theta}{\tau_t} \quad (2)$$

where θ is the shortest angle between \mathbf{g} and \mathbf{A} , and τ_t is the time constant for tilt. (2) The perceptual system interprets the GIA in the logical way, as partially or wholly due to the presence of gravity, with any remaining portion indicating linear acceleration in the given direction. In other words,

$$\mathbf{a} = \mathbf{A} - \mathbf{g} \quad (3)$$

where \mathbf{a} and \mathbf{g} are the perceptual estimates of \mathbf{a}_A and \mathbf{g}_A , respectively. These principles allow the cone perception to be explained in words: because \mathbf{A} rotates slowly about the subject during slow OVAR, \mathbf{g} follows it by Eq. 2 and therefore rotates, creating a perceived cone (Fig. 1b). Also, the cylinder can be explained in words: fast rotation causes \mathbf{A} to keep changing direction on a time scale shorter than τ_t , precluding significant time for change in \mathbf{g} . Because \mathbf{g} is relatively fixed, the perceived linear acceleration, \mathbf{a} , rotates along with \mathbf{A} by Eq. 3, creating a cylindrical motion (Fig. 1c).

At first glance, these explanations seem to make sense; the underlying principles are part of the foundation of modern three-dimensional modeling. The first principle (Graybiel and Brown 1951) is called the somatogravic or oculogravic illusion depending on the nature of the measurement technique used (Clark and Graybiel 1966; Curthoys 1996) and is a well-established property of perception and its modeling (Mayne 1974). The second principle has been termed the GIF-resolution hypothesis and has been demonstrated experimentally (Angelaki et al. 2004; Merfeld 1995a; Merfeld et al. 1993, 1999).

A surprising and little-known fact is that these principles actually fail to predict the shape of most subjects' perceptions, particularly the cone. Although variations other than the bottom-pivot cone have been reported, the bottom-pivot cone is the most common. Denise et al. (1988) reported that 23 of 27 experienced a bottom-pivot cone with the summit or apex located from the waist to 2-m below the feet. In more recent studies by Wood et al. (including 2007), only one of 28 subjects reported the apex above the head (top-pivot), 4 of 28 reported an apex between their feet and chest (bottom-pivot), while the remaining 23 of 28 reported bottom-pivot cone with apex at or below their feet. As will be described in the Sect. 4, the standard models that use the principles listed above predict a top-pivot cone. This fact can be shown by mathematical analysis of the consequences of the principles (details in Sects. 4, 5). We also present computed examples. The crux of the reason is that the relative phases of perceived tilt and translation according to the standard model (i.e., a model governed by these principles) cannot match that of a bottom-pivot cone as in Fig. 1b. The mathematical analysis will show, in fact, that the predicted phase difference between perceived tilt and perceived translation from equations like these will always produce a shape closer to a top-pivot cone, regardless of the values of parameters such as time constants. This shape/phase difficulty is a problem for understanding perception in three dimensions. One goal of this article is to seek an explanation for the commonly reported bottom-pivot cone motion.

For this study, we assume that vectors for angular acceleration and linear acceleration, detected by the vestibular and other sensory systems, are continuously available to the perceptual system. This study addresses the question by what operations these vectors are used to produce a perception. As shown here—by both computational models and mathematical proof—the

operations are not just those in the “standard” model; several alternative hypotheses are tested. While the somatosensory system contributes to the central vestibular system’s estimate of angular and linear accelerations, it is also more diffuse and contributes additionally to self-motion perception in other ways. Although the total accelerations are physically the same regardless of whether they affect the somatosensory or vestibular system, somatosensory receptors are distributed in such a way that forces can also be detected at specific points of the body. More pressure at a certain point, such as the head or feet, can cue the perceptual system and lead to different perceptions, as has been found to happen for barbecue spit rotation (Lackner and Graybiel 1978). In other words, that pressure can give a context within which the perceptual system interprets the ongoing whole-body angular and linear accelerations. It is not currently known whether differently distributed somatosensory pressure or attention would produce different perceptions; that has not been the focus of the OVAR studies cited here. However, this issue is discussed further in Sect. 5, about whether the context may play a role in the perceptual system’s “choice” of how to process the angular and linear accelerations. Of course, within a given context, it is a scientific question how the whole-body angular and linear acceleration vectors are used to produce the perception, whether using time constants, vector differences, or otherwise. That is the focus of this article: How are the angular and linear acceleration vectors used to produce the perception? This article concentrates on the most common perception, the bottom-pivot cone shape with phase reversal.

The shape/phase difficulty does not arise for eye movements. First, eye movements are not always associated with a unique shape of motion because the same types of eye movements can compensate for either translation or rotation. Second, the phase responses of eye movements and perceptions dissociate during variable radius centrifugation (Park et al. 2006) and during OVAR (Wood et al. 2007). In fact, eye movements are enough different from perception that models based upon the above principles have been able to successfully predict components of human eye movements during OVAR (Bockisch et al. 2003; Fanelli et al. 1990; Hain 1986; Haslwanter et al. 2000; Kushiro et al. 2002; Merfeld 1995a; Raphan and Schnabolk 1988; Schnabolk and Raphan 1992). The more direct neural pathways for eye movements may give different responses than those for perception, in which a wider set of pathways and previous experience or expectations are likely to be important factors (Wertheim et al. 2001).

Models aiming to predict perception, on the other hand, have been able to predict selected aspects of the motion such as the tilt and horizontal angular velocity components (Droulez and Darlot 1989), the amplitude of tilt and translation (Vingerhoets et al. 2006), or the amplitude and phase of tilt (Laurens and Droulez 2007), though not necessarily the cone shape, which requires in-phase tilt and translation. One model (Droulez and Darlot 1989) was able to predict the necessary in-phase tilt and translation, consistent with a cone; however, the same model’s results for oscillatory head translation predicted out of phase tilt and translation, and in general, the model had the capacity for numerical instability in some cases (Reymond et al. 2002). For a newer version (Reymond et al. 2002), only barbecue-spit rotation and only tilt phase results have been presented, while another model (Zupan et al. 2002) resulted in barbecue-spit tilt and translation components out of phase. In summary, current models have yet to display all the necessary relationships between components for a cone-shaped perception during OVAR.

A similar shape/phase difficulty also exists for horizontal linear oscillation (Glasauer 1995). During horizontal linear oscillation, for example interaural while upright, subjects typically report the “hilltop illusion”: side-to-side translation with oscillating roll tilt so that the shape of the motion is as though moving side to side over a hill, with the amount of tilt depending on the frequency and amplitude of the linear acceleration (Glasauer 1995). Despite word explanations for the perception, the known principles of self-motion perception fail to predict the hilltop illusion, for reasons similar to the shape/phase difficulty in OVAR. In particular,

the above principles predict that tilt phase will change substantially with frequency, and that tilt and translation will be out of phase. Therefore, to explain the hilltop illusion, a non-linear predictive mechanism has been proposed instead (Glasauer 1995).

Self-motion perception may take advantage of the wide variety of central neuron responses in a way different from that for eye movements. Differences between perception and eye movements are not too surprising when considering the central physiology. While vestibular-related eye movements and self-motion perception share sensory endorgans, much of their central processing differs. The vestibulo-ocular reflex, in its simplest form, involves a three-neuron arc (reviewed in Goldberg and Fernández 1984) with primary afferents, secondary neurons in the vestibular nuclei, and motor neurons. Self-motion perception, on the other hand, involves many neural centers, including the vestibular nuclei, other parts of the brain stem (Brandt et al. 2002; Dieterich and Brandt 1993), the thalamus (Anastasopoulos and Bronstein 1999; Brandt et al. 2002; Hawrylyshyn et al. 1978), and areas of the cortex such as the temporal lobe and the parieto-insular cortex (Baloh and Halmagyi 1996; Bottini et al. 1994; Brandt and Dieterich 1999; Brandt et al. 1994, 2002; Fredrickson et al. 1966; Miyamoto et al. 2005; Takeda et al. 1995). In addition, perception and eye movements have been shown to be differentially affected by proprioceptive input (Mergner et al. 1998).

For oscillatory motions, a variety of neuron response phases has been shown experimentally in central neurons (Angelaki and Dickman 2000; Angelaki et al. 2004; Dickman and Angelaki 2002, 2004; Perlmutter et al. 1999; Schor et al. 1998), making the identification of different linear-angular motions possible (Holly et al. 1999, 2006). This wide range of phases can allow perception and eye movements to differ, because the nervous system has available a variety of neuron responses that can give tilt and translation phases that are most appropriate for perception. Convergence between neurons with different response phases would allow any necessary phase and amplitude relationship (Angelaki 1991, 1992; Angelaki et al. 1993). However, for OVAR, most existing models do not yet correctly predict the shape of three-dimensional perception, much less give the central underpinnings.

The goal of this article is to develop further principles that allow the correct prediction of the shape of three-dimensional perception during OVAR, by investigating existing principles and identifying missing pieces. The first step involves implementing the “Standard Model” consisting of the core of current models, as explained in detail in Sect. 2. The mismatches between the Standard Model’s predictions and the typical subject perception are made more easily identifiable by enhancement of the model with a three-dimensional display, a method that has been successful in the past to explain perceptions in centrifuges (Holly 1997, 2000) and during head movements while rotating (Holly 2003, 2004). The goal is to use mathematical analysis to identify shortcomings in the current scientific understanding of perception, and then to develop a new model based upon additional principles for self-motion perception, testing the new model with both OVAR and horizontal oscillation. In addition, computation allows comparison with examples of the Standard Model.

2 Models and hypotheses

The development, testing, and proof were carried out by a sequence of steps:

1. implementation of the Standard Model (described below) enhanced by three-dimensional display, for slow ($45^\circ/\text{s}$) OVAR,
2. generation of new principles and hypotheses based upon identification of differences between the Standard Model and typical subject perceptions for slow OVAR,
3. tests of the new hypotheses/models for slow ($45^\circ/\text{s}$) OVAR,

4. tests of the Standard Model and new hypotheses/models for fast (180°/s) OVAR,
5. tests of the Standard Model and new hypotheses/models for slow and fast horizontal linear oscillation,
6. mathematical proof of the behavior of Standard Model.

Used here were the standard (Hixson et al. 1966) head coordinates with x noseward, y leftward, and z head-upward. Angular velocity and acceleration are specified using the right-hand rule. So that non-zero velocities are correctly registered, variables such as velocity and acceleration are implemented in a coordinate system that is head-coincident (Holly 1996)—i.e., the coordinate axes are always instantaneously Earth-fixed but positioned and oriented with those of the head—rather than head-fixed, which may move with respect to the Earth.

2.1 Standard Model

Certain principles underlie the vast majority of three-dimensional computational models of perception and eye movements. The common themes are (1) the laws of physics and (2) certain well-known tendencies of the nervous system. The fact that the nervous system essentially understands the physical relationships between position, velocity, and acceleration forms the foundation of three-dimensional models, and is sometimes phrased in terms of separate properties such as velocity storage, GIF-resolution, canal-otolith interaction, etc. (Bockisch et al. 2003; Borah et al. 1988; Bos and Bles 2002; Droulez and Darlot 1989; Haslwanter et al. 2000; Kushiro et al. 2002; Mayne 1974; Merfeld 1995a,b; Merfeld et al. 1993; Ormsby and Young 1977; Raymond et al. 2002; Zupan et al. 2002), or the nervous system's understanding of the laws of physics can be viewed en bloc (Holly 1997, 2000).

Superimposed upon the laws of physics are tendencies unique to the nervous system, the most well established falling into categories of angular, linear, and tilt (Guedry 1974). The well-known angular tendency is for perceived angular velocity, ω , to decrease over time in the absence of new angular acceleration α (Eq. 1). This tendency can be phrased and implemented in a variety of ways, whether through leaky integration, incomplete velocity storage, partial feedback, outcome of Kalman filtering, priors in Bayesian modeling, or time constants in transfer functions or differential equations. For linear motion, the same type of tendency holds, though with a much shorter time constant (Seidman et al. 1998a). Perceived linear velocity, \mathbf{v} , decreases over time based upon perceived linear acceleration, \mathbf{a} :

$$\frac{d\mathbf{v}}{dt} = \mathbf{a} - \frac{\mathbf{v}}{\tau_1} \quad (4)$$

where τ_1 is the time constant of decay of linear velocity.

For tilt, the tendency is for the perceived earth-upward “gravity” vector, \mathbf{g} , in subject coordinates to move toward the GIA, \mathbf{A} , as explained in Sect. 1 and Eq. 2. At the same time, \mathbf{g} is affected by perceived angular velocity, ω , by a cross product relationship standard in physics and three-dimensional perception modeling,

$$\frac{d\mathbf{g}}{dt} = \mathbf{g} \times \omega$$

which is then modified by the tendency toward \mathbf{A} as follows. In three-dimensions, the angle θ between \mathbf{A} and \mathbf{g} is

$$\theta = \cos^{-1} \left(\frac{\mathbf{A} \cdot \mathbf{g}}{\|\mathbf{A}\| \|\mathbf{g}\|} \right)$$

and a unit vector in the direction in which a subject’s angular velocity would rotate \mathbf{g} most directly toward \mathbf{A} is

$$\mathbf{u} = \frac{\mathbf{A} \times \mathbf{g}}{\|\mathbf{A} \times \mathbf{g}\|}$$

noting that \mathbf{g} is in subject coordinates and roughly earth-fixed, so it moves in the opposite direction from the subject’s rotation. Letting

$$f(\mathbf{A}, \mathbf{g}) = \theta \mathbf{u} \tag{5}$$

the resulting final equation governing perceived tilt is

$$\frac{d\mathbf{g}}{dt} = \mathbf{g} \times \left(\omega + \frac{\mathbf{f}(\mathbf{A}, \mathbf{g})}{\tau_t} \right) \tag{6}$$

where τ_t is the time constant for tilt of \mathbf{g} toward \mathbf{A} . It is alternatively possible to consider the possibility that \mathbf{g} is drawn more quickly toward \mathbf{A} when \mathbf{A} has large magnitude, for example by defining

$$f(\mathbf{A}, \mathbf{g}) = \theta (\mathbf{A} \times \mathbf{g}) \tag{7}$$

and adjusting the time constant accordingly. However, it is not clear from experimental research whether Eq. 5 or 7 is a better choice, and because \mathbf{A} has constant magnitude during OVAR, the more straightforward version, (5), is used here.

There is also a question of the nervous system’s implementation of the tilt tendency, as well as the GIF-resolution hypothesis ($\mathbf{A} = \mathbf{a} + \mathbf{g}$, or equivalently, Eq. 3). Again, the perceptual tendency can be implemented in a variety of ways, including those listed above for the angular- and linear-velocity tendencies. For tilt- and the GIF-resolution hypothesis, the feedback method is sometimes phrased in terms of error signals. For example (Merfeld and Zupan 2002), the sum of (perceived) \mathbf{a} and \mathbf{g} can be compared with the stimulus, \mathbf{A} ; the difference can then be considered an “error” used to adjust \mathbf{a} and \mathbf{g} through appropriate feedback loops. The vector \mathbf{g} tends toward \mathbf{A} , and the linear acceleration, \mathbf{a} , ends up being computed, in effect, by

$$\mathbf{a} = c(\mathbf{A} - \mathbf{g}) \tag{8}$$

where c is a gain constant < 1 . For the purposes of analyzing phases in OVAR, the choice of gain constant is immaterial, so the Standard Model in this article uses straightforward GIF resolution, Eq. 3.

This common foundation governs the overall behavior of most three-dimensional models and computer simulations of perception and eye movements. The qualitative results, therefore, are similar from one model to the next, because the models share the same equations, including

the same angular/linear/tilt tendencies. The differences lie not in the global behavior but in the details, due to differences in exact values of parameters, input and output variables, and in specialized components designed to predict specific phenomena. One example is a supplemental otolith estimate of angular velocity (Kushiro et al. 2002) designed in relation to the bias in horizontal eye movements. Such a component is not included here because it is less standard and does not affect the shape of perceived motions. Another special feature is explicit frequency-segregation of linear acceleration, using low-pass filters for tilt and high-pass filters for translation. The use of the time constants τ_t and τ_l can accomplish this filtering implicitly (Merfeld et al. 2005a; Merfeld and Zupan 2002).

In this article, this core of physics and tendencies is called the Standard Model (Fig. 2). Again, the choice of implementation, whether leaky integration, feedback, etc., is immaterial for the global behavior. Added to the standard calculations were those for a position reference, \mathbf{p} , and heading as given by \mathbf{i} and \mathbf{j} and computed in a way consistent with that for \mathbf{g} . The values for the time constants τ_a , τ_l , and τ_t were selected to match perceptions in slow OVAR. In other words, simulations of slow OVAR were carried out with different values for the time constants, and the values that led to the best match with known experimental results were selected. The value of τ_a is the most well-known experimentally (Guedry et al. 1971; Mittelstaedt and Mittelstaedt 1996), having a value around 20 s, and was tested here with 10, 20, and 50 s. The value of τ_l is considered quite small (Seidman et al. 1998a), and was tested here with 0.1, 0.5, and 5 s; these refer to the time constant for perception, not the shorter time constant associated with the mechanical properties of the sensory structures (Grant and Best 1987). The value of τ_t is considered to be on the order of 5 s (Curthoys 1996; Seidman et al. 1998b) or less (Bos and Bles 2002; Merfeld et al. 2001), and was tested with 0.1, 0.5, 5, and 10 s. Although the exact values do not substantially affect the basic shape of perceived motion, the values $\tau_a = 20$ s, $\tau_l = 0.5$ s, and $\tau_t = 0.5$ s were chosen as the best match with slow OVAR perception (details in Sect. 4), and were used throughout the rest of the article. Additional calculations were performed with all combinations of extreme time constant values 4 and 100 s for τ_a , 0.01 and 20 s for τ_l , and 0.1 and 20 s for τ_t , to more fully test the technical limitations of the Standard Model.

2.2 Alternative hypotheses/models

Three additional hypotheses were considered (Fig. 2b–d):

Hypothesis #1. Horizontal oscillatory translation is reversed.

Hypothesis #2. Translation is phase-linked to tilt.

Hypothesis #3. Tilt is phase-linked to translation.

The motivation for these three hypotheses stemmed from the Standard Model results, as presented in Sect. 4, showing that the Standard Model does not predict in-phase tilt and translation as required by a bottom-pivot cone. Hypothesis #1 was motivated by experimental findings that an oscillatory translational component of perception can be reversed to match other sensory input. In particular, vertical oscillation has been shown to be perceived with reversed phase to be consistent with visual input (Wright et al. 2005). In OVAR, it is the horizontal translation that is oscillatory, so Hypothesis #1 specifies horizontal translation as reversed. Hypotheses #2 and #3 are two alternatives that also use as much of the Standard Model as possible. Because many aspects of the Standard Model are well accepted, the three hypotheses are chosen to deviate as little as possible from known properties of perception, as given in Sect. 2.1.

Hypothesis #1, that horizontal translation is reversed, was implemented by taking the Standard Model's computation of linear acceleration and reversing the subjective earth-horizontal

component (Fig. 2b). The goal is for the oscillatory component to be reversed in perception, and this was technically carried out by extracting horizontal and vertical components. From the Standard Model's computed perceived linear acceleration, $\mathbf{a}_s (= \mathbf{A} - \mathbf{g})$, the vector was broken into its (perceived) vertical and horizontal components,

$$\mathbf{a}_s = \mathbf{a}_{\text{vert}} + \mathbf{a}_{\text{horiz}}$$

and perceived linear acceleration was then computed as

$$\mathbf{a} = \mathbf{a}_{\text{vert}} - \mathbf{a}_{\text{horiz}}$$

The preservation of the vertical component represented the recognition of direction relative to gravity. This computation, in effect, reversed the phase of the predicted perceived translation.

Hypothesis #2, that translation is phase-linked to tilt, was implemented by replacing the Standard Model's computation of linear velocity with a computation that linked the direction of linear velocity with the direction of tilt (Fig. 2c). For example, rightward roll velocity would imply rightward linear velocity; forward pitch velocity would imply forward linear velocity, etc., implemented by

$$\mathbf{v} = (\boldsymbol{\omega}_{\text{tilt}} \times \mathbf{k}_h) s$$

where $\boldsymbol{\omega}_{\text{tilt}}$ is the (perceived) earth-horizontal component of $\boldsymbol{\omega}$, \mathbf{k}_h is a unit vector in the head's z direction, and s is a scale factor. This model kept the Standard Model's computation of tilt.

Hypothesis #3, that tilt is phase-linked to translation (Fig. 2d), is the opposite of Hypothesis #2. Tilt velocity is determined by the direction of linear velocity. For example, rightward linear velocity would imply a rightward roll velocity; forward linear velocity would imply forward pitch velocity, etc. Such a model keeps the Standard Model's computation of translation, and replaces its computation of tilt. This hypothesis could also be written technically with a cross product but was implemented only conceptually, for reasons explained in Sect. 4.

2.3 Computer implementation

The equations for all models were programmed in a manner to make available all three-dimensional position and orientation output, with \mathbf{i} , \mathbf{j} , \mathbf{g} , and \mathbf{p} (Fig. 2). This three-dimensional information was fed into three-dimensional displays to view the shape of the predicted perceived motion.

The software for model implementation was developed in Matlab (The MathWorks, Inc. Natick, Massachusetts, USA). Simultaneous differential equations were solved using the Runge-Kutta 45 algorithm. Three-dimensional graphical display software was also developed in Matlab, using the output of the model simulations. The simulations were performed on Macintosh computers with PowerPC and Intel processors. Additional testing with real-time motion display was performed using programs developed in Persistence of Vision Ray Tracer (POV-Ray, www.povray.org) using the Matlab output along with a Perl (LarryWall, www.perl.com or www.cpan.org) script custom-written for automated POV-Ray code generation.

3 Data and conventions

For OVAR, peer-reviewed experimental results were used for testing the hypotheses. Denise et al. (1988) tested subjects at 45°/s rotation and angles up to 30° tilt, and found that 23 of 27 subjects perceived a bottom-pivot cone. Wood et al. (2007) found that at 45°/s rotation and 20° tilt, 11 of 14 subjects perceived a conical path. At 45°/s rotation and 10° tilt, 14 of 14 subjects perceived a conical path. At 180°/s rotation and 20° tilt, 9 of 11 subjects perceived cylindrical path, while 2 perceived a tight cone. For tilt phase, Wood et al. (2007) found perceptual tilt phase lags typically between 0° and 30° relative to the GIA, when subjects used a joystick to continuously report motion. Perceived translation also lagged the GIA typically between 0° and 30°. Wood et al. (2007) found that a push-button method of reporting pitch showed phase leads of around 15°, while Denise et al. (1988) reported phase leads between 0° and 50°, also using a push-button method. In all cases, phase responses varied widely between subjects.

This study focused on OVAR with 20° tilt and rotation at either 45°/s (slow OVAR) or 180°/s (fast OVAR). The rotation was considered clockwise as viewed from the top of the head; therefore, the GIA rotated in a counterclockwise direction relative to the head. Based upon the experimental results discussed above and other published experimental research, typical subject reports were taken to be a perception of conical motion (Fig. 1b) progressing counterclockwise (Denise et al. 1988; Guedry 1974; Vingerhoets et al. 2006; Wood et al. 2007). The perceived tilt and translation were, therefore, in phase. In other words, the tilt-back orientation coincided with the furthest back translated position. The phase of reported tilt was taken to be near zero; i.e., perceived tilt-back orientation coincided with actual tilt-back orientation. Such reports are, however, highly variable in phase as discussed above, and appear to depend upon the method of reporting, showing phase leads when the timing of specific orientations are reported by the push of a button (Benson et al. 1975; Denise et al. 1988) or phase lags when orientation is continuously reported by a joystick (Wood et al. 2007), so the exact phase of perceived tilt relative to actual tilt was taken to be less important than the perceived in-phase tilt and translation as indicated by subject reports of conical motion.

Most important in the comparison is the shape of the motion, quantified by phase relationships. The actual motion's tilt is used as a reference for phase measurements. Phases are denoted by

$$\begin{aligned}\phi_T &= \text{phase of perceived tilt relative to actual tilt,} \\ \phi_L &= \text{phase of perceived translation relative to actual tilt, and} \\ \phi &= \phi_L - \phi_T.\end{aligned}$$

Positive ϕ_T means that the perceived tilt-back orientation occurred before (led) the actual tilt-back orientation. Positive ϕ_L means that the perceived furthest back position occurred before (led) the actual tilt-back orientation. The shape of three-dimensional perception is tied to the difference, ϕ , rather than to the absolute phases. In particular, a bottom-pivot cone (Fig. 1b) is produced when $\phi = 0^\circ$. A top-pivot cone, with the pivot above the head, would be produced if $\phi = \pm 180^\circ$. For $0^\circ < \phi < 180^\circ$, more complicated motions occur. For $\phi = 90^\circ$ or $\phi = 270^\circ$, the motion would be essentially cylindrical but with either the feet or the head angling into the direction of motion, leading the body around the cylinder.

For the simulations, \mathbf{A} was taken to move in the same way as undergone by subjects,

$$\mathbf{A} = \begin{bmatrix} g \sin \theta \cos wt \\ -g \sin \theta \sin wt \\ g \cos \theta \end{bmatrix} \quad (9)$$

where $g = 9.81 \text{ m/s}^2$, $\theta = 20^\circ$, w is the actual angular velocity, and t is time. Also, angular acceleration $\mathbf{a} = \mathbf{0}$ as undergone by subjects in a previous study (Wood et al. 2007). Initial conditions were set as veridical during the constant-velocity rotation. The purpose of the study is to investigate the perceptions that arise after start-up effects have decayed, so simulations were carried out until the predicted perception had stabilized into a periodic motion.

For horizontal linear oscillation (with upright subject), the classic “hilltop illusion”, e.g., as reported by Glasauer (1995) was used for comparison with the models. In other words, subjective perception was considered to be side-to-side translation with oscillating roll tilt so that the shape of the motion was as though moving side to side over a hill. Although this type of report is also variable and dependent upon the frequency of oscillation (with even greater variability at very small angle oscillations of the GIA Wertheim et al. 2001), the hilltop motion is a typical perception, sometimes occurring more horizontally with tilts at the ends. Frequency and GIA angle were chosen to match that for the slow and fast OVAR simulations, with $45^\circ/\text{s}$ ($1/8\text{Hz}$) and $180^\circ/\text{s}$ ($1/2\text{Hz}$) oscillations in which \mathbf{A} reached a maximum angle of 20° relative to vertical at the endpoints of motion. As in the OVAR simulations, $\mathbf{a} = \mathbf{0}$, and the magnitude and angle of \mathbf{A} were taken to match those undergone by subjects:

$$\mathbf{A} = \begin{bmatrix} 0 \\ M \sin(2\pi ft) \\ g \end{bmatrix}$$

where $M = 3.57 \text{ m/s}^2 (= g \tan 20^\circ)$ and $f = 1/8$ and $1/2$. In this case, \mathbf{A} not only changed direction relative to the head, but also changed periodically in magnitude during the course of the oscillation.

4 Results

4.1 Slow OVAR: test of Standard Model

For the Standard Model (Fig. 2), the time constants chosen were $\tau_a = 20 \text{ s}$, $\tau_l = 0.5\text{s}$, and $\tau_t = 0.5\text{s}$. These choices were based upon matching the most common slow ($45^\circ/\text{s}$) OVAR perception, for which ϕ_T is desired in the general vicinity of zero. The initial computation with $\tau_a = 20\text{s}$, $\tau_l = 0.5\text{s}$, and $\tau_t = 5\text{s}$ resulted in $\phi_T = -76^\circ$. Variations of τ_a had little effect on ϕ_T , with $\tau_a = 10\text{s}$ and $\tau_a = 50\text{s}$ giving $\phi_T = -76^\circ$ and $\phi_T = -73^\circ$, respectively. Variations of τ_l did not affect ϕ_T . Variations of τ_t did affect ϕ_T , with $\tau_t = 0.1\text{s}$, 0.5 , 5 (again), and 10 s giving $\phi_T = -4.5^\circ$, -21° , -76° , and -86° , respectively. The value $\tau_t = 0.5\text{s}$ was chosen as being the most consistent with the small values found in pure GIA-tilt experiments (Bos and Bles 2002; Merfeld et al. 2001) and phase lags averaging in a range $<30^\circ$ during slow OVAR (Wood et al. 2007), taking into consideration the wide range of subjective responses found experimentally (Benson et al. 1975; Denise et al. 1988; Wood et al. 2007). Tests with extreme values showed that ϕ_T could not reach zero, but was always negative, consistent with the OVAR model of Laurens and Droulez (2007) and the tilt-translation model of Park et al. (2006). The translation phase, ϕ_L , was always large and far from ϕ_T ; both ϕ_L and $\phi (= \phi_L - \phi_T)$ were always $>90^\circ$. Therefore, ϕ_L was not considered in choosing time constants because a different mechanism would be necessary to match the translation phase.

Standard Model simulations of slow OVAR resulted in a counterclockwise top-pivot cone (Fig. 3). Though similar to subject reports in the general shape of a cone, and in moving counterclockwise, the cone had pivot above the head. Also, in conjunction with the top-pivot position, the results gave $\phi = 158^\circ$, relatively near 180° . In addition, although experimental data are not currently available on perceived vertical motion, the simulation showed constant downward motion.

4.2 Slow OVAR: new hypotheses

Three alternative hypotheses were developed here (Fig. 2b–d) to explain the frequent subjective perception of a bottom-pivot cone (Denise et al. 1988; Guedry 1974; Vingerhoets et al. 2006; Wood et al. 2007), rather than the near top-pivot cone predicted by the Standard Model:

- #1 Translation phase is reversed in perception during OVAR.
- #2 Translation is phase-linked, i.e., put into phase, with the Standard Model's tilt in perception during OVAR.
- #3 Tilt is phase-linked to the Standard Model's translation in perception during OVAR.

In testing Hypothesis #1 by reversing the phase of translation (Fig. 2b), the result was a bottom-pivot cone with $\phi = -22^\circ$ (Fig. 4a–c). A continuous downward motion still appeared, however.

The result of testing Hypothesis #2 by phase-linking translation to tilt (Fig. 2c) was also a bottom-pivot cone with $\phi = 0^\circ$ (Fig. 4d–f). For phase-linking, a scale factor must be chosen to relate translational position and tilt angle; here, the scale factor was chosen to correspond to a pivot 2-m below the head, implemented by $s=2$ in the model (Fig. 2c). Other scale factors could be chosen, corresponding to intersubject differences, but the same basic cone shape would still arise. No downward motion appeared in the phase-link simulation.

Hypothesis #3 was tested conceptually by considering phase-linking tilt to translation (Fig. 2d) and was found not to require further testing by simulation. In particular, the desired bottom-pivot cone would indeed be obtained because $\phi = 0^\circ$ by in-phase tilt and translation. However, the phase of translation, ϕ_L , would match that of the Standard Model, by definition of the hypothesis, and the Standard Model's ϕ_L was always $>90^\circ$ as explained in Sect. 4.1. Such a large ϕ_L is inconsistent with the experimental data which shows phase nearer 0° (described in Sect. 3). Therefore, Hypothesis #3 did not require further testing.

Based upon the simulations with alternative hypotheses, Hypotheses #1 and #2 are supported, but Hypothesis #3 is not. It is worth noting that all the three simulations—Standard Model, Reverse Translation, and Phase-Link translation to tilt—show a small amount of precession (slightly different angles of overlaid gray and white heads in Fig. 3d, Fig. 4a, d).

4.3 Fast OVAR: test of hypotheses

For fast ($180^\circ/s$) OVAR, simulations of the Standard Model and the models for Hypotheses #1 and #2 gave circular counterclockwise motion (Fig. 5) of smaller radius than that for slow OVAR (Fig. 3, Fig. 4). The Standard Model's circular motion had tilt with the bottom of the head slightly leading the circular motion with $\phi = 126^\circ$. The reverse-translation (#1) hypothesis' circular motion had tilt with the bottom of the head slightly lagging the circular motion with $\phi = -54^\circ$. The phase-link-to-tilt (#2) hypothesis' circular motion had tilt so that the shape was a bottom-pivot cone with $\phi = 0^\circ$, though with less tilt (Fig. 5i) than for slow OVAR (Fig. 4f). Both the Standard Model (Fig. 5a–c) and the Hypothesis #1 with reversed translation (Fig. 5d–f) gave constant downward motion, while Hypothesis #2 linking translation to tilt (Fig. 5g–i) did not have downward motion.

Again, Hypothesis #3 linking tilt to translation was tested conceptually and eliminated. In particular, the Standard Model's ϕ_L was $>90^\circ$ (Fig. 5c), causing the cone's phase for Hypothesis #3 to be inconsistent with experimental data showing phase near 0° .

The best match with experimental findings was given by Hypothesis #2 linking translation to tilt. Notably, not only did the bottom-pivot cone result from phase-linking translation with tilt, but also the tilt was less than for slow OVAR, supporting the possibility that many subjects

may feel this faster, less-tilted motion as simply cylindrical, while a few subjects may report perception of a tight cone, just as reported experimentally (Wood et al. 2007). Technically, the model would need a tilt perception threshold implemented to display the pure cylinder. This is a simple modification, and was additionally tested with success (figure not shown, but is the same as in Fig. 5g, h though with the head always upright).

4.4 Linear oscillation: test of hypotheses

For horizontal interaural linear translation, the Standard Model and the models for Hypotheses #1 and #2 were tested. All simulations gave periodic interaural movement (Fig. 6). Both the Standard Model (Fig. 6a, b) and the Hypothesis #1 with reversed translation (Fig. 6c, d) gave simultaneous constant upward motion, while Hypothesis #2 linking translation to tilt (Fig. 6e, f) had periodic vertical motion in phase with the tilt, as though over a hill. For slow (1/8Hz) oscillation, the Standard Model's motion snaked upward with horizontal translation about 180° out of phase with tilt (Fig. 6). In addition, the translation was almost opposite in phase with the actual translation. For fast (1/2Hz) oscillation, the Standard Model's motion also had horizontal translation more than 90° out of phase with tilt (not shown). The reverse translation (#1) hypothesis' motion also snaked upward in both the cases, but with translation more closely in phase with tilt. The phase-link-to-tilt (#2) hypothesis' motion had translation and tilt in phase, for both slow oscillation (Fig. 6) and fast oscillation (not shown).

The best match with experimental findings was given Hypothesis #2 phase-linking translation to tilt, which gave the hilltop shape.

4.5 Proof that the standard model cannot predict a bottom-pivot cone

Why does the Standard Model fail to predict a bottom-pivot cone for OVAR, and can parameters be adjusted to predict a bottom-pivot cone? The model can be further investigated analytically. We demonstrate that the Standard Model cannot predict a bottom-pivot cone for any parameter values. The demonstration is based on the two principles given in Sect. 1.

The main point is that any linear model will produce a phase lag in perceived tilt ($\phi_T < 0$), and the phase lag will cause a phase lead in perceived translation ($\phi_L > 0$) by GIF resolution (Eq. 3 or 8). More thorough determination of the values of ϕ_T and ϕ_L is made possible here by the fact that actual tilt is only 20°, so small-angle approximations allow derivation and analytical solution for ϕ_T and ϕ_L . First, the head-horizontal projection of \mathbf{A} (Eq. 9) is

$$\mathbf{A}_{xy} = \begin{bmatrix} \mathbf{A}_x \\ \mathbf{A}_y \end{bmatrix} = A \begin{bmatrix} \cos wt \\ \sin wt \end{bmatrix} \quad (10)$$

where $A = g \sin 20^\circ$ here. The tendency of \mathbf{g} to move toward alignment with \mathbf{A} by Eq. 2 or equivalently, 6, can be approximated under these relatively upright circumstances, using the small-angle approximation $\theta \approx \sin \theta$, as a tendency for the head-horizontal projection \mathbf{g}_{xy} of \mathbf{g} to approach \mathbf{A}_{xy} by

$$\frac{d\mathbf{g}_{xy}}{dt} = \frac{\mathbf{A}_{xy} - \mathbf{g}_{xy}}{\tau}$$

where $\tau = g\tau_t$, with $g = 9.81 \text{ m/s}^2$.

The values of ϕ_T and ϕ_L are then obtained by solving the differential equations

$$\begin{aligned}\frac{dg_x}{dt} &= \frac{1}{\tau} (A \cos wt - g_x) \\ \frac{dg_y}{dt} &= \frac{1}{\tau} (A \sin wt - g_y)\end{aligned}$$

to which the solutions are

$$\begin{aligned}g_x &= \frac{A}{1+w^2\tau^2} (\cos wt + wt \sin wt) + c_1 e^{-t/\tau} \\ g_y &= \frac{A}{1+w^2\tau^2} (\sin wt - wt \cos wt) + c_2 e^{-t/\tau}\end{aligned}\quad (11)$$

where c_1 and c_2 are constants that depend on the initial conditions. As $t \rightarrow \infty$, the exponential terms go to zero, and through the use of sine and cosine addition formulas, the long-term solution can be written

$$\mathbf{g}_{xy} = \frac{A}{\sqrt{1+w^2\tau^2}} \begin{bmatrix} \cos(wt + \phi_T) \\ \sin(wt + \phi_T) \end{bmatrix}$$

where

$$\phi_T = \tan^{-1}(-w\tau) = \tan^{-1}(-wg\tau_l).$$

Therefore,

$$-90^\circ < \phi_T < 0^\circ$$

and perceived tilt exhibits a phase lag with value closest to 0° for small w .

The simultaneous head-horizontal linear acceleration is obtained by combining Eqs. 10 and 11 as $t \rightarrow 0$:

$$\begin{aligned}\mathbf{a}_{xy} &= \mathbf{A}_{xy} - \mathbf{g}_{xy} \\ &= A \begin{bmatrix} \cos wt \\ \sin wt \end{bmatrix} - \frac{A}{1+w^2\tau^2} \begin{bmatrix} \cos wt + wt \sin wt \\ \sin wt - wt \cos wt \end{bmatrix} \\ &= \frac{Aw\tau}{1+w^2\tau^2} \begin{bmatrix} w\tau \cos wt - \sin wt \\ w\tau \sin wt + \cos wt \end{bmatrix} \\ &= w\tau \begin{bmatrix} -g_y \\ g_x \end{bmatrix} \\ &= \frac{Aw\tau}{\sqrt{1+w^2\tau^2}} \begin{bmatrix} \cos(wt + (\phi_T + 90^\circ)) \\ \sin(wt + (\phi_T + 90^\circ)) \end{bmatrix}\end{aligned}\quad (12)$$

with the last step obtained through the use of sine and cosine addition formulas. Therefore, \mathbf{a}_{xy} leads \mathbf{g}_{xy} by 90° .

If \mathbf{a}_{xy} were integrated perfectly twice to obtain perceived translation, the conclusion would be that $\phi_L = \phi_T + 90^\circ$ and $0^\circ < \phi_L < 90^\circ$. However, the integration is imperfect (Eq. 4). The projection of perceived linear velocity, \mathbf{v} , to the head xy -plane is given by

$$\frac{d\mathbf{v}_{xy}}{dt} = \mathbf{a}_{xy} - \frac{\mathbf{v}_{xy}}{\tau_l} \quad (13)$$

with \mathbf{a}_{xy} from 12. Solving 13 and omitting negligible terms for large t gives solution

$$\mathbf{v}_{xy} = \frac{Aw\tau_l}{(1+w^2\tau_l^2)\sqrt{1+w^2\tau_l^2}} \times \begin{bmatrix} \cos(wt+\phi_T+90^\circ)+w\tau_l\sin(wt+\phi_T+90^\circ) \\ \sin(wt+\phi_T+90^\circ) - w\tau_l\cos(wt+\phi_T+90^\circ) \end{bmatrix}$$

Integrating \mathbf{v}_{xy} and flipping signs to obtain the center, \mathbf{c} , of the circumscribed circle relative to the head at all times, in head coordinates, the result is

$$\mathbf{c} = \frac{Ag\tau_l\tau_l}{\sqrt{1+w^2\tau_l^2}\sqrt{1+w^2(g\tau_l)^2}} \begin{bmatrix} \cos(wt+\phi_L) \\ \sin(wt+\phi_L) \end{bmatrix}$$

where

$$\phi_L = \phi_T + 90^\circ + \tan^{-1}\left(\frac{1}{w\tau_l}\right).$$

Therefore, the phase difference, $\phi = \phi_L - \phi_T$, between translation and tilt has

$$90^\circ < \phi < 180^\circ$$

with greater values for smaller angular velocities, w .

In summary, the Standard Model (or any linear model with similar properties) cannot predict a bottom-pivot cone, $\phi = 0^\circ$. Instead, the slower the rotation, the more the Standard Model predicts a top-pivot cone, $\phi = 180^\circ$.

4.6 Summary of results

The hypothesis of explicit phase-linking of translation to tilt (Hypothesis #2) can explain results of perception during OVAR and horizontal linear oscillation. The Standard Model cannot explain the perceived motion, even though it encompasses the laws of physics and basic tendencies of the nervous system.

5 Discussion

This investigation demonstrates that phase-linking of translation to tilt in perception may explain human perception of self-motion during periodic motions. The Standard Model, alone, predicts a phase relationship that differs strongly from that perceived in OVAR, as proved mathematically here, and in the hilltop illusion, as shown by Glasauer (1995) through simulation of components and shown here by three-dimensional display. The addition of phase-linking, on the other hand, reproduces the most common perception during both of these periodic motions, in which translation is perceived in phase with tilt. The following sections

discuss the models and possible explanations for the tendencies of perception, then consider the existence of neuronal mechanisms.

5.1 Relationship to other models

The model that results from this study differs from most other models in two main respects: the present model includes a three-dimensional display along with all aspects of every component of the motion, and the present model specifically aims to model the perceived motion, since perception differs from eye movements. However, this model shares a foundation with many models, in the laws of physics and certain well-known tendencies of the nervous system, incorporated here in a Standard Model. This foundation along with carefully tuned additional features have been successful previously in predicting various components of perception, such as the tilt and the horizontal angular velocity components (Droulez and Darlot 1989), the amplitude and phase of tilt and translation (Vingerhoets et al. 2006), and the amplitude and phase of tilt (Laurens and Droulez 2007).

In order to predict a cone motion, the relative phases ϕ_T of tilt and ϕ_L of translation are salient, and were specifically studied in this work. A mathematical approach is used here to formally analyze the Standard Model. In addition, the three-dimensional display allows confirmation of the three-dimensional perception. The Standard Model, and therefore models with that foundation, predicts $\phi (= \phi_L - \phi_T) > 90^\circ$. For $45^\circ/s^2$ OVAR at 20° tilt, ϕ is near 180° , corresponding most closely to a top-pivot perception, as experienced by only a small percentage of subjects (Denise et al. 1988). Therefore, a new hypothesis, phase-linking, is shown to reproduce the majority, bottom-pivot cone perception. The analysis shows that the results would hold for other OVAR tilt angles between 0° and 90° . Preliminary testing with a 30° angle gave very similar results to the 20° angle.

One feature of some three-dimensional models (Droulez and Darlot 1989; Mayne 1974; Paige and Seidman 1999; Seidman et al. 1998b; Telford et al. 1997) that is not explicitly shown in the current model is frequency segregation of linear input. These other models display a high-pass filter for translation and a low-pass filter for tilt—thereby also having a frequency effect on perceived angular motion. In the current Standard Model, the time constants τ_l and τ_t accomplish frequency segregation implicitly (Merfeld et al. 2005a; Merfeld and Zupan 2002). In this sense, the current model has filters analogous to those in models with linear low-pass and high-pass filters. In addition, the current model has the linear– angular interaction necessary for motions with angular motion about a non-vertical axis (Kaptein and Van Gisbergen 2006). Indeed, frequency segregation alone has been shown to be incompatible with results on the time course of OVAR perception (Vingerhoets et al. 2006). Nevertheless, additional explicit filtering may be necessary for a more general model (Bockisch et al. 2003; Haslwanter et al. 2000). However, even with the prospect of additional explicit filtering, the present research shows that linear mechanisms such as linear filters do not suffice to accomplish phase-linking, so non-linear mechanisms are necessary instead.

For horizontal oscillation and the hilltop illusion, the most closely related model involves a non-linear predictive mechanism (Glasauer 1995). This model complements the present research, because it covers a range of frequencies and gives a method for keeping the hilltop motion's phase in line with experimental results which show little phase shift over frequencies. In the Standard Model, such a phase match over a range of frequencies would have to be accomplished by changes in the tilt time constant τ_t . The non-linear predictive mechanism gives a uniform means of accomplishing the phase match, and also matches amplitude of tilt. The present research makes fuller and more accurate predictions by giving the full set of motion components, not only for tilt but also for translation and the relative phase between tilt and translation, as well as a view of the vertical component.

5.2 Forces and motion

This study began with simulation of a physical movement, as a perfect accelerometer would measure it, plus the uncontroversial addition of time constants for angular, linear, and tilt motion. However, perception of the OVAR and the hilltop illusion requires the addition of another perceptual property: phase-linking. Why would nervous systems potentially obscure veridical perception by imposing phase-linking? This question is ill-posed; it assumes a sort of omniscience on the part of the nervous system, whereas in fact movement sensation is a biological process carried out in sensory organs. Each responds to physical events; none provides a complete representation of the physical movement. Whether a motion is active and/or involves limb movements such as in bicycling, or is passive and involves motion of the body as a whole such as in OVAR and horizontal linear oscillation, nervous systems are capable of combining the responses of sensory organs to construct an overall motion perception, guided by perceptual principles. The nervous system has available to it through various sensory systems information about acceleration, or equivalently, total force on the body, and even about the distribution of forces by means of the somatosensory system. For OVAR as investigated here, the relationship between force and motion may give insight into the perceptions.

One factor during OVAR may be the direction of total force (or equivalently, sensed acceleration) on the subject. During OVAR, the GIA, \mathbf{A} , is earth-vertical. During perceived conical motion, the GIA as detected by the sensors may be in the perceived earth-vertical direction or at an angle, depending upon the perceived angle of tilt. For the top-pivot cone predicted by the Standard Model and for the bottom-pivot cone predicted by phase-linking, the detected GIA is nearly earth-upward (Fig. 7). One difference between the top-pivot and bottom-pivot cones is that from the reference frame of the *angled body's* longitudinal axis, the detected GIA points away from the rotation axis in the top-pivot cone (Fig. 7a), and points toward the rotation axis in the bottom-pivot cone (Fig. 7b).

The somatosensory system is one of the systems that senses the GIA (Fig. 7), by means of total force on the body. However, the somatosensory system can also sense the distribution of forces on the body surface and torques at the joints, which are not studied in most OVAR research. Nevertheless, the distribution of forces may be relevant for perception, as they are in barbecue-spit rotation (OVAR with a horizontal axis): during barbecue-spit rotation, subjects perceive a conical motion with pivot at the head or feet depending upon whether they apply pressure on the apparatus with the head or with the feet (Lackner and Graybiel 1978). For OVAR as investigated here, with a diagonally tilted axis, the dependence of perception on the distribution of forces is a potential topic for future research. One possibility is that somatosensory cues or individual attention patterns affect the context in which the perceptual system enters a phase-linking state.

The difference between top- and bottom-pivots can also be viewed another way in terms of the frames of reference. A bottom-pivot may be related to lesser motion of the feet, similar to that experienced when standing on a fixed floor. It may be that subjects who retain the top-pivot perception focus on the force as it is applied to the body, rather than on the vertex of the cone. In any case, choice of a frame of reference is common in perception. For example, in visual perception a large or otherwise dominant object is chosen as a frame of reference (Rock 1997). The auditory cocktail party problem involves choosing a frame of reference in a hubbub. The vestibular nuclei, which are central to self-motion perception, display conditional shifts in neural frames of reference, depending on whether a head movement is passive or active (Boyle et al. 1996; McCollum and Boyle 2001; McCrea et al. 1999; Roy and Cullen 2001).

5.3 Explanation according to familiarity

The top-pivot cone may be rejected by perception, which may instead be governed by a principle that perception tends toward familiar motions. Perception may seek a familiar motion that is as consistent as possible with the laws of physics and basic tendencies of the nervous system. A subject who perceives a bottom-pivot cone may be tending toward lesser motion of the feet, angular, and linear motions being linked as they are during natural tilts of the upper body, and/or having the GIA point, relative to the body axis, inward toward the rotation axis, as occurs in many cases of actual rotation (Fig. 7b).

The explanation that perception tends toward familiar motions is applied here to complex motions, but is an extension of a long-standing principle for simple motions. Many well-known facts about perception stem from this principle. For example, subjects feel stationary during sustained rotation in the dark, a perception that presumably stems from the fact that stationarity is the most common state encountered in natural conditions, among those states that match the ongoing stimulus. In addition, subjects tend to interpret the GIA as vertical because the most common state with sustained linear force is that with the force being vertical, due to gravity. The concept that perception is influenced by prior knowledge is the foundation of Bayesian models (Laurens and Droulez 2007), and is often used in coding explanations of nervous system function (reviewed in Pouget et al. 2003; Averbeck et al. 2006).

The concept of familiarity has also been applied to perception in a centrifuge. For centrifuges, a “whole-motion” model has been developed to take into account the way in which angular and linear vectors interact during familiar motions, predicting experimentally reported perceptions of self-motion (Holly and Harmon 2009; Holly et al. 2008). This view of motion as a whole is the same concept presented by phase-linking: during whole motion in everyday life, angular and linear components often coincide in certain ways. In fact, the phase-linking concept can be considered an extension, for oscillatory motion, of the whole-motion model.

In the case of OVAR, another clue to familiar perception and the cone can be found at the beginning of the rotation. At the beginning, subjects report veridical rotation (Vingerhoets et al. 2006), but in everyday experience such a rotation would occur naturally while rolling (in yaw) on a surface, i.e., with translation. If this familiar translation begins to arise in OVAR subjects’ (mis)perceptions, then the translation would turn into a conical motion as the angular stimulus subsides. This is another way to appeal to everyday experience to explain the cone perception. The influence of everyday experience may explain certain previously observed principles, that the linear and the angular components of complex motion perception are interdependent, and that perception at a given time depends strongly on perceptions leading to that point (Holly and McCollum 1996).

A propensity for phase-linked motion has also been demonstrated in bimanual voluntary movements (Cohen 1971; Kelso 1984; Kelso et al. 1981). This phase-linking has been shown to originate on a perceptual-cognitive level rather than arising from homologous muscle pairs (Mechsner 2004). In addition, in-phase motions are preferred over anti-phase motions (Mechsner 2004).

Perception of translation seems to be particularly labile. In this study on OVAR and horizontal oscillation, the timing of perceived horizontal translation was shown to match that of the tilt predicted by the tendency to align \mathbf{g} with \mathbf{A} (i.e., the tilt given by the Standard Model). In other words, translation (as given by \mathbf{p} in Fig. 2) was determined by tilt (as given by the angle of \mathbf{g}) rather than by the usual principles as implemented in the Standard Model with GIF-resolution (Fig. 2a). In other research, translation has been shown to be similarly misperceived and affected by other stimuli. During vertical linear oscillation with a visual scene oscillation of comparable amplitude but of opposite phase, the perceived direction of motion was typically

governed by the visual scene, not the physical oscillation (Wright et al. 2005). In other words, the perceived translation was in phase with the visual scene, and out of phase with the actual translation. This is like the familiar uncertainty one often has in an elevator about whether it is moving up or down. In fact, perceived translation in general may be more governed by non-directional cues such as vibration and sound than by linear accelerations, as shown during horizontal linear motion (Yong et al. 2007). The fact that translation perception is influenced so strongly by other cues lends additional credence to the idea that perceived translation would be phase-linked to tilt rather than the other way around.

A strength of the explanation according to familiarity is that it explains the perceptions during both the OVAR and the hilltop illusion. A disadvantage to the nervous system is that perception works best when it is capable of distinguishing between motions. Subjects may differ in the amount to which they appeal to familiar perceptions, i.e., how many equivalence classes of motions their perceptual systems admit. In any case, many subjects perceive highly unfamiliar motions, such as the shank stretch reported by Lackner and DiZio (1988). The tendency to appeal to familiarity in the case of the GIA reverting to vertical may be due to overlooking other possible explanations; this example and phase-linking may be explainable by a privileged role of gravitation in self-motion perception.

5.4 Explanations that emphasize sensorimotor processes and neural organization

Gravitation is one major factor in sensorimotor learning from birth. As a force, it supplies a relationship between position and duration; as any object falls, it moves faster, according to gravitational acceleration. It is true that nervous systems must construct a simulacrum of such a relationship for predictive purposes. However, this is such an omnipresent relationship that a substrate for it may be hard-wired.

The three-dimensionality of physical space is similarly extremely familiar, so that it could presumably be learnt from the time of early eye or head movements. The same is true of the horizontal plane. However, these geometrical structures are hard-wired or have strong physiological substrates in the vestibular system and its projections, as analyzed using the mathematics of symmetry groups (Foster et al. 2007; McCollum 2007; McCollum and Boyle 2004). These geometrical structures are spatial; the geometrical structure of gravitation is both spatial and temporal.

It is not known whether gravitation is hard-wired in nervous systems, but we do know that the relationships involved in gravitational acceleration are learnt from the time subjects hold up their heads. Learning during early development may be stronger, in terms of later perceptions, than later learning.

One case in which the learning of gravitation has been studied is in the acquisition of independent locomotion. It has been suggested that physical principles are acquired one at a time in early locomotion (Bril and Brenière 1993). If, as children learn to walk in the first week or two, they are integrating different laws of motion, then their forms of locomotion will differ. Integrating the laws of conservation of angular momentum, linear momentum, or energy lead to three distinct forms of locomotion (McCollum et al. 1995). A longitudinal study of early locomotion has found that children indeed use these three differing forms (Snapp-Childs and Corbetta 2005). The importance of locomotion in human development suggests that the familiarity of gravitation may have a special place in perception because of the way it is learnt.

At the systemic level of the organism where perception occurs, contributions from multiple neural centers are combined to construct a perception, involving other factors in addition to gravity. Although humans are clearly capable of perceiving three-dimensional, non-phase-linked motions, in all the cases analyzed here, there is a preference for phase-linked perceptions.

This preference may arise from the contributions of neural centers with neurons that tend to be responsive to position, velocity, and/or acceleration all in the same direction. Such neurons occur for vestibular stimuli in the ventral intraparietal area (VIP) of the cerebral cortex (Klam 2004). Similar neurons occur in the middle temporal area (MT) for visual stimuli (Albright 1989); a tendency to perceive phase-linking visually could bias eyes-closed motion perception. Grossberg et al. (1999) present an argument that perceptual tendencies in the cerebral cortex arise from intrinsic cortical architecture.

Neural propensity in the vestibular nuclei leads to the choice of a fixed frame of reference for movements (Boyle et al. 1996; McCollum and Boyle 2001; McCrea et al. 1999; Roy and Cullen 2001). If the propensity to choose some fixed frame of reference operates in OVAR, evidently the feet are chosen to move less than the head, in the bottom-pivot cone.

5.5 Neuronal mechanisms

The proposed principles can be implemented by neurons that are known to exist in the nervous system. Although the actual mechanisms are unknown, a demonstration of the possibility of phase-linking is given here. Previous OVAR models have shown that detection of a rotating linear vector can be accomplished by time-delayed coordination of neuron responses to linear acceleration (Fanelli et al. 1990; Raphan and Schnabolk 1988; Schnabolk and Raphan 1992). This detection of a rotating vector could also be accomplished by a coordination of responses from neurons whose phases are shifted relative to one another. Such neurons have been found to exist in the vestibular nuclei (Angelaki et al. 1993; Schor et al. 1985), so the coordination could happen through subsequent convergence. In particular, a strong total response to rotation would occur upon convergence from a set of vestibular nuclei neurons with a range of preferred response directions in a circle in the horizontal plane, if neurons further around the circle respond with greater phase leads (or lesser phase lags). The relationship between recorded central neuron responses and computational models has begun to be explored for tilt–translation combinations (Angelaki et al. 2004; Green and Angelaki 2004).

Upon detection of periodic motion, phase-linking of perceived tilt and translation could be accomplished by parallel input from neurons whose responses are roughly in phase with the motion itself. Such neurons are known to exist at the secondary level, as a full range of response phases—both lead and lag—and preferred directions are possible through convergence (Angelaki 1991, 1992; Angelaki et al. 1993; Schor et al. 1985). The switch to phase-linking is essentially context-specific, and context-specific adaptation is already known to exist in the vestibular system, as seen at both the behavioral level (Baker et al. 1987; Nashner et al. 1982; Shelhamer et al. 1992) and the neuron level (Boyle et al. 1996; McCollum and Boyle 2001; McCrea et al. 1999; Roy and Cullen 2001).

In summary, the necessary components for periodic-motion phase-linking are already known to exist in the nervous system. The above method is one way to implement, with neurons, a non-linear predictive mechanism.

5.6 Conclusion

Shown here is that phase-linking, as a property of the neural construction of self-motion perception, applies to both OVAR and horizontal linear acceleration. The phase-linking property may plausibly be explained according to some combination of familiarity, gravitation, development, and neural propensity. As self-motion perception is investigated in increasingly complicated motions, research will be facilitated by viewing motions as a whole in three dimensions. In addition, the consideration of principles of self-motion perception such as phase-linking is expected to be crucial to understanding the way perceptions are constructed.

Acknowledgments

This research was supported by National Institutes of Health Grants R15-DC008311 (to JEH) and R01-DC04794 (to GM), Colby College Natural Sciences Division Annual Grants (to JEH), and the National Space Biomedical Research Institute through NASA NCC 9-58 (NA405 to SJW).

References

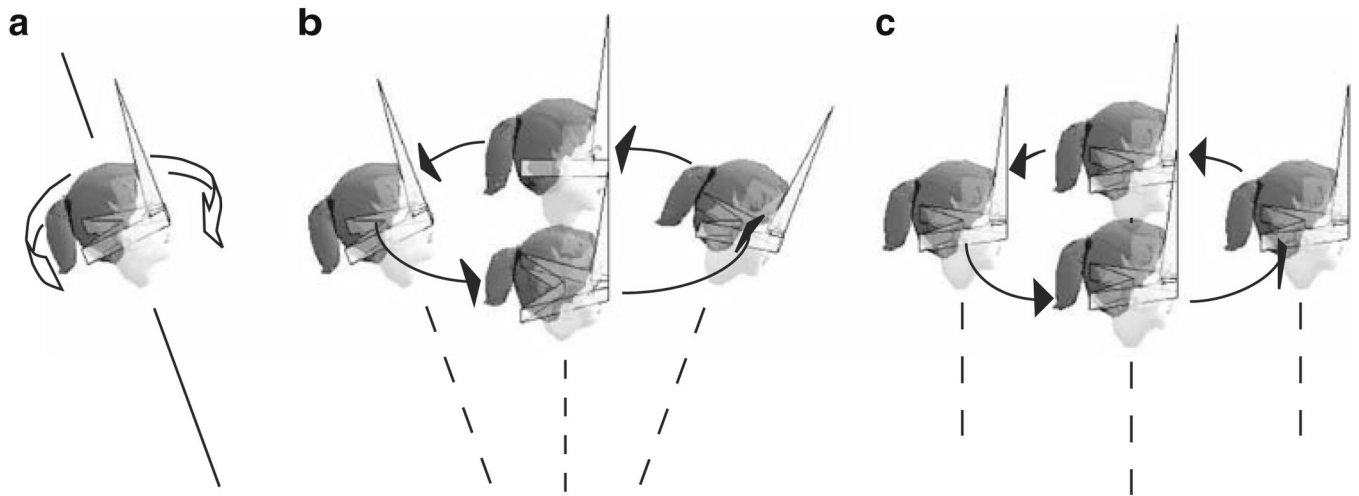
- Albright TD. Centrifugal directional bias in the middle temporal visual area (MT) of the macaque. *Vis Neurosci* 1989;2:177–188. [PubMed: 2487646]
- Anastasopoulos D, Bronstein AM. A case of thalamic syndrome: somatosensory influences on visual orientation. *J Neurol Neurosurg Psychiatry* 1999;67:390–394. [PubMed: 10449566]
- Angelaki DE. Dynamic polarization vector of spatially tuned neurons. *IEEE Trans Biomed Eng* 1991;38:1053–1060. [PubMed: 1748439]
- Angelaki DE. Spatio-temporal convergence (STC) in otolith neurons. *Biol Cybern* 1992;67:83–96. [PubMed: 1606247]
- Angelaki DE, Dickman JD. Spatiotemporal processing of linear acceleration: primary afferent and central vestibular neuron responses. *J Neurophysiol* 2000;84:2113–2132. [PubMed: 11024100]
- Angelaki DE, Bush GA, Perachio AA. Two-dimensional spatio-temporal coding of linear acceleration in vestibular nuclei neurons. *J Neurosci* 1993;13:1403–1417. [PubMed: 8463828]
- Angelaki DE, Shaikh AG, Green AM, Dickman JD. Neurons compute internal models of the physical laws of motion. *Nature* 2004;430:560–564. [PubMed: 15282606]
- Averbeck BB, Latham PE, Pouget A. Neural correlations, population coding and computation. *Nat Rev Neurosci* 2006;7:358–366. [PubMed: 16760916]
- Baker JF, Perlmutter SI, Peterson BW, Rude SA, Robinson FR. Simultaneous opposing adaptive changes in cat vestibulo-ocular reflex direction for two body orientations. *Exp Brain Res* 1987;69:220–224. [PubMed: 3436390]
- Baloh, RW.; Halmagyi, GM. Disorders of the vestibular system. Oxford: Oxford University Press; 1996.
- Benson AJ, Diaz E, Farrugia P. The perception of body orientation relative to a rotating linear acceleration vector. *Fortschr Zool* 1975;23:264–274. [PubMed: 1116815]
- Bockisch CJ, Straumann D, Haslwanter T. Eye movements during multi-axis whole-body rotations. *J Neurophysiol* 2003;89:355–366. [PubMed: 12522185]
- Borah J, Young LR, Curry RE. Optimal estimator model for human spatial orientation. *Ann N Y Acad Sci* 1988;545:51–73. [PubMed: 3071213]
- Bos JE, Bles W. Theoretical considerations on canal-otolith interaction and an observer model. *Biol Cybern* 2002;86:191–207. [PubMed: 12068786]
- Bottini G, Sterzi R, Paulesu E, Vallar G, Cappa SF, Erminio F, Passingham RE, Frith CD, Frackowiak RS. Identification of the central vestibular projections in man: a positron emission tomography activation study. *Exp Brain Res* 1994;99:164–169. [PubMed: 7925790]
- Boyle R, Belton T, McCrea RA. Responses of identified vestibulospinal neurons to voluntary eye and head movements in the squirrel monkey. *Ann N Y Acad Sci* 1996;781:244–263. [PubMed: 8694418]
- Brandt T, Dieterich M. The vestibular cortex. Its locations, functions, and disorders. *Ann N Y Acad Sci* 1999;871:293–312. [PubMed: 10372080]
- Brandt T, Dieterich M, Danek A. Vestibular cortex lesions affect the perception of verticality. *Ann Neurol* 1994;35:403–412. [PubMed: 8154866]
- Brandt T, Glasauer S, Dieterich M. Vestibular brainstem disorders: clinical syndromes in roll plane and their model simulation. *Mov Disord* 2002;17 Suppl 2:S58–S62. [PubMed: 11836757]
- Bril, B.; Brenière, Y. Posture and independent locomotion in early childhood: learning to walk or learning postural dynamic control?. In: Savelsbergh, GJP., editor. *The development of coordination in infancy*. Amsterdam: Elsevier; 1993. p. 337-358.
- Clark B, Graybiel A. Factors contributing to the delay in the perception of the oculogravic illusion. *Am J Psychol* 1966;79:377–388. [PubMed: 5968474]
- Cohen L. Synchronous bimanual movements performed by homologous and non-homologous muscles. *Percept Mot Skills* 1971;32:639–644. [PubMed: 5089097]

- Correia MJ, Guedry FE Jr. Modification of vestibular responses as a function of rate of rotation about an Earth-horizontal axis. *Acta Otolaryngol* 1966;62:297–308. [PubMed: 5297305]
- Curthoys IS. The delay of the oculogravic illusion. *Brain Res Bull* 1996;40:407–412. [PubMed: 8886366]
- Denise P, Darlot C, Droulez J, Cohen B, Berthoz A. Motion perceptions induced by off-vertical axis rotation (OVAR) at small angles of tilt. *Exp Brain Res* 1988;73:106–114. [PubMed: 3208851]
- Dickman JD, Angelaki DE. Vestibular convergence patterns in vestibular nuclei neurons of alert primates. *J Neurophysiol* 2002;88:3518–3533. [PubMed: 12466465]
- Dickman JD, Angelaki DE. Dynamics of vestibular neurons during rotational motion in alert rhesus monkeys. *Exp Brain Res* 2004;155:91–101. [PubMed: 15064889]
- Dieterich M, Brandt T. Ocular torsion and tilt of subjective visual vertical are sensitive brainstem signs. *Ann Neurol* 1993;33:292–299. [PubMed: 8498813]
- Droulez, J.; Darlot, C. The geometric and dynamic implications of the coherence constraints in three-dimensional sensorimotor interactions. In: Jeannerod, M., editor. *Attention and performance*. Hillsdale: Lawrence Erlbaum; 1989. p. 495-526.
- Fanelli R, Raphan T, Schnabolk C. Neural network modeling of eye compensation during off-vertical-axis rotation. *Neural Netw* 1990;3:265–276.
- Fernández C, Goldberg JM. Physiology of peripheral neurons innervating semicircular canals of the squirrel monkey. II. Response to sinusoidal stimulation and dynamics of peripheral vestibular system. *J Neurophysiol* 1971;34:661–675. [PubMed: 5000363]
- Foster IZ, Hanes DA, Barmack NH, McCollum G. Spatial symmetries in vestibular projections to the uvula-nodulus. *Biol Cybern* 2007;96:439–453. [PubMed: 17205298]
- Fredrickson JM, Scheid P, Figge U, Kornhuber HH. Vestibular nerve projection to the cerebral cortex of the rhesus monkey. *Exp Brain Res* 1966;2:318–327. [PubMed: 4959658]
- Glasauer S. Linear acceleration perception: frequency dependence of the hilltop illusion. *Acta Otolaryngol Suppl* 1995;520:37–40. [PubMed: 8749075]
- Goldberg, JM.; Fernández, C. The vestibular system. In: Darian-Smith, I., editor. *The nervous system*. Vol. vol III. Bethesda: American Physiological Society; 1984. p. 977-1022.
- Grant W, Best W. Otolith-organ mechanics: lumped parameter model and dynamic response. *Aviat Space Environ Med* 1987;58:970–976. [PubMed: 3314853]
- Graybiel A, Brown R. The delay in visual reorientation following exposure to a change in direction of resultant force on a human centrifuge. *J Gen Psychol* 1951;45:143–150.
- Green AM, Angelaki DE. An integrative neural network for detecting inertial motion and head orientation. *J Neurophysiol* 2004;92:905–925. [PubMed: 15056677]
- Grossberg S, Mingolla E, Pack C. A neural model of motion processing and visual navigation by cortical area MST. *Cereb Cortex* 1999;9:878–895. [PubMed: 10601006]
- Guedry, FE, Jr. Psychophysics of vestibular sensation. In: Kornhuber, HH., editor. *Vestibular system*. Part 2: psychophysics and applied aspects and general interpretations. Vol. vol VI/2. Berlin: Springer; 1974. p. 3-154.
- Guedry FE Jr, Stockwell CW, Gilson RD. Comparison of subjective responses to semicircular canal stimulation produced by rotation about different axes. *Acta Otolaryngol* 1971;72:101–106. [PubMed: 5095486]
- Guedry FE, Rupert AH, McGrath BJ, Oman CM. The dynamics of spatial orientation during complex and changing linear and angular acceleration. *J Vestib Res* 1992;2:259–283. [PubMed: 1342402]
- Hain TC. A model of the nystagmus induced by off vertical axis rotation. *Biol Cybern* 1986;54:337–350. [PubMed: 3741902]
- Haslwanter T, Jaeger R, Mayr S, Fetter M. Three-dimensional eye-movement responses to off-vertical axis rotations in humans. *Exp Brain Res* 2000;134:96–106. [PubMed: 11026731]
- Hawrylyshyn PA, Rubin AM, Tasker RR, Organ LW, Fredrickson JM. Vestibulothalamic projections in man—a sixth primary sensory pathway. *J Neurophysiol* 1978;41:394–401. [PubMed: 306422]
- Hixson, WC.; Niven, JL.; Correia, MJ. Monograph 14. Pensacola: Naval Aerospace Medical Institute; 1966. Kinematics nomenclature for physiological accelerations.
- Holly JE. Subject-coincident coordinate systems and sustained motions. *Int J Theor Phys* 1996;35:445–473.

- Holly JE. Three-dimensional baselines for perceived self-motion during acceleration and deceleration in a centrifuge. *J Vestib Res* 1997;7:45–61. [PubMed: 9057159]
- Holly JE. Baselines for three-dimensional perception of combined linear and angular self-motion with changing rotational axis. *J Vestib Res* 2000;10:163–178. [PubMed: 11354430]
- Holly JE. Perceptual disturbances predicted in zero-g through three-dimensional modeling. *J Vestib Res* 2003;13:173–186. [PubMed: 15096662]
- Holly JE. Vestibular coriolis effect differences modeled with three-dimensional linear-angular interactions. *J Vestib Res* 2004;14:443–460. [PubMed: 15735327]
- Holly JE, Harmon KJ. Spatial disorientation in gondola centrifuges predicted by the form of motion as a whole in 3-D. *Aviat Space Environ Med* 2009;80:125–134. [PubMed: 19198199]
- Holly JE, McCollum G. The shape of self-motion perception—II. Framework and principles for simple and complex motion. *Neuroscience* 1996;70:487–513. [PubMed: 8848155]
- Holly JE, McCollum G, Boyle R. Identification of head motions by central vestibular neurons receiving linear and angular input. *Biol Cybern* 1999;81:177–188. [PubMed: 10473843]
- Holly JE, Pierce SE, McCollum G. Head tilt-translation combinations distinguished at the level of neurons. *Biol Cybern* 2006;95:311–326. [PubMed: 16944195]
- Holly JE, Vrubleviskis A, Carlson LE. Whole-motion model of perception during forward- and backward-facing centrifuge runs. *J Vestib Res* 2008;18:171–186. [PubMed: 19208962]
- Kaptein RG, Van Gisbergen JA. Canal and otolith contributions to visual orientation constancy during sinusoidal roll rotation. *J Neurophysiol* 2006;95:1936–1948. [PubMed: 16319209]
- Kelso JA. Phase transitions and critical behavior in human bimanual coordination. *Am J Physiol* 1984;246:R1000–R1004. [PubMed: 6742155]
- Kelso JA, Holt KG, Rubin P, Kugler PN. Patterns of human interlimb coordination emerge from the properties of non-linear, limit cycle oscillatory processes: theory and data. *J Mot Behav* 1981;13:226–261. [PubMed: 15215072]
- Klam, F. Ph.D. Collège de France. Paris, France: University Paris VI; 2004. Head movement-related signals and the representation of space in parietal cortex: an electrophysiological study with awake behaving monkeys.
- Kushiro K, Dai M, Kunin M, Yakushin SB, Cohen B, Raphan T. Compensatory and orienting eye movements induced by off-vertical axis rotation (OVAR) in monkeys. *J Neurophysiol* 2002;88:2445–2462. [PubMed: 12424285]
- Lackner JR, DiZio P. Visual stimulation affects the perception of voluntary leg movements during walking. *Perception* 1988;17:71–80. [PubMed: 3205672]
- Lackner JR, Graybiel A. Some influences of touch and pressure cues on human spatial orientation. *Aviat Space Environ Med* 1978;49:798–804. [PubMed: 656007]
- Laurens J, Droulez J. Bayesian processing of vestibular information. *Biol Cybern* 2007;96:389–404. [PubMed: 17146661]
- Mayne, R. A systems concept of the vestibular organs. In: Kornhuber, HH., editor. *Vestibular system. Part 2: psychophysics and applied aspects and general interpretations. Vol. vol VI.* Berlin: Springer; 1974. p. 493-580.
- McCollum G. Spatial symmetry groups as sensorimotor guidelines. *J Vestib Res* 2007;17:347–359. [PubMed: 18626144]
- McCollum G, Boyle R. Conditional transitions in gaze dynamics: role of vestibular nuclei in eye-only and eye/head gaze behaviors. *Biol Cybern* 2001;85:423–436. [PubMed: 11762233]
- McCollum G, Boyle R. Rotations in a vertebrate setting: evaluation of the symmetry group of the disynaptic canal-neck projection. *Biol Cybern* 2004;90:203–217. [PubMed: 15052483]
- McCollum G, Holroyd C, Castelfranco AM. Forms of early walking. *J Theor Biol* 1995;176:373–390. [PubMed: 8538217]
- McCrea RA, Gdowski GT, Boyle R, Belton T. Firing behavior of vestibular neurons during active and passive head movements: vestibulo-spinal and other non-eye-movement related neurons. *J Neurophysiol* 1999;82:416–428. [PubMed: 10400968]

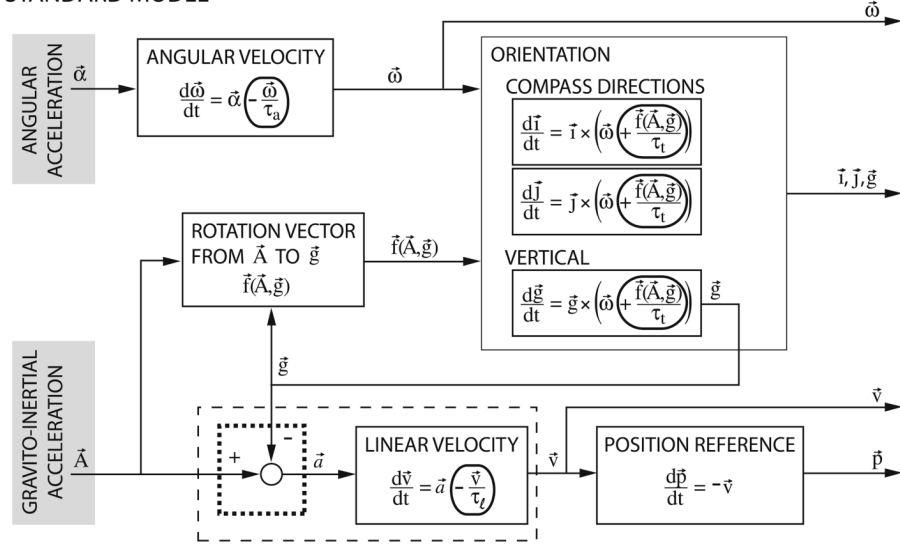
- McGrath BJ, Guedry FE, Oman CM, Rupert AH. Vestibulo-ocular response of human subjects seated in a pivoting support system during 3Gz centrifuge stimulation. *J Vestib Res* 1995;5:331–347. [PubMed: 8528475]
- Mechner F. A psychological approach to human voluntary movements. *J Mot Behav* 2004;36:355–370. [PubMed: 15695214]
- Merfeld DM, Zupan LH. Neural processing of gravito-inertial cues in humans. III. Modeling tilt and translation responses. *J Neurophysiol* 2002;87:819–833. [PubMed: 11826049]
- Merfeld DM, Young LR, Oman CM, Shelhamer MJ. A multidimensional model of the effect of gravity on the spatial orientation of the monkey. *J Vestib Res* 1993;3:141–161. [PubMed: 8275250]
- Merfeld DM, Zupan L, Peterka RJ. Humans use internal models to estimate gravity and linear acceleration. *Nature* 1999;398:615–618. [PubMed: 10217143]
- Merfeld DM. Modeling human vestibular responses during eccentric rotation and off vertical axis rotation. *Acta Otolaryngol Suppl* 1995a;520:354–359. [PubMed: 8749160]
- Merfeld DM. Modeling the vestibulo-ocular reflex of the squirrel monkey during eccentric rotation and roll tilt. *Exp Brain Res* 1995b;106:123–134. [PubMed: 8542968]
- Merfeld DM, Zupan LH, Gifford CA. Neural processing of gravito-inertial cues in humans. II. Influence of the semicircular canals during eccentric rotation. *J Neurophysiol* 2001;85:1648–1660. [PubMed: 11287488]
- Merfeld DM, Park S, Gianna-Poulin C, Black FO, Wood S. Vestibular perception and action employ qualitatively different mechanisms. I. Frequency response of VOR and perceptual responses during translation and tilt. *J Neurophysiol* 2005a;94:186–198. [PubMed: 15728767]
- Merfeld DM, Park S, Gianna-Poulin C, Black FO, Wood S. Vestibular perception and action employ qualitatively different mechanisms. II. VOR and perceptual responses during combined tilt and translation. *J Neurophysiol* 2005b;94:199–205. [PubMed: 15730979]
- Mergner T, Schweigart G, Botti F, Lehmann A. Eye movements evoked by proprioceptive stimulation along the body axis in humans. *Exp Brain Res* 1998;120:450–460. [PubMed: 9655230]
- Mittelstaedt ML, Jensen W. Centrifugal force affects perception but not nystagmus in passive rotation. *Ann N Y Acad Sci* 1999;871:435–438. [PubMed: 10372099]
- Mittelstaedt ML, Mittelstaedt H. The influence of otoliths and somatic graviceptors on angular velocity estimation. *J Vestib Res* 1996;6:355–366. [PubMed: 8887892]
- Miyamoto T, Fukushima K, Takada T, De Waele C, Vidal PP. Saccular projections in the human cerebral cortex. *Ann N Y Acad Sci* 2005;1039:124–131. [PubMed: 15826967]
- Nashner LM, Black FO, Wall C III. Adaptation to altered support and visual conditions during stance: patients with vestibular deficits. *J Neurosci* 1982;2:536–544. [PubMed: 6978930]
- Ormsby CC, Young LR. Integration of semicircular canal and otolith information for multisensory orientation stimuli. *Math Biosci* 1977;34:1–21.
- Paige GD, Seidman SH. Characteristics of the VOR in response to linear acceleration. *Ann N Y Acad Sci* 1999;871:123–135. [PubMed: 10372066]
- Park S, Gianna-Poulin C, Black FO, Wood S, Merfeld DM. Roll rotation cues influence roll tilt perception assayed using a somato-sensory technique. *J Neurophysiol* 2006;96:486–491. [PubMed: 16571732]
- Perlmutter SI, Iwamoto Y, Baker JF, Peterson BW. Spatial alignment of rotational and static tilt responses of vestibulospinal neurons in the cat. *J Neurophysiol* 1999;82:855–862. [PubMed: 10444682]
- Pouget A, Dayan P, Zemel RS. Inference and computation with population codes. *Annu Rev Neurosci* 2003;26:381–410. [PubMed: 12704222]
- Raphan T, Schnabolk C. Modeling slow phase velocity generation during off-vertical axis rotation. *Ann N Y Acad Sci* 1988;545:29–50. [PubMed: 3149166]
- Reymond G, Droulez J, Kemeny A. Visuovestibular perception of self-motion modeled as a dynamic optimization process. *Biol Cybern* 2002;87:301–314. [PubMed: 12386745]
- Rock, I. The perception of movement. In: Rock, I.; Palmer, S., editors. *Indirect perception*. Cambridge: MIT Press; 1997. p. 209–247.
- Roy JE, Cullen KE. Selective processing of vestibular reafference during self-generated head motion. *J Neurosci* 2001;21:2131–2142. [PubMed: 11245697]

- Schnabolk C, Raphan T. Modeling 3-D slow phase velocity estimation during off-vertical-axis rotation (OVAR). *J Vestib Res* 1992;2:1–14. [PubMed: 1342381]
- Schor RH, Miller AD, Timerick SJ, Tomko DL. Responses to head tilt in cat central vestibular neurons. II. Frequency dependence of neural response vectors. *J Neurophysiol* 1985;53:1444–1452. [PubMed: 3874267]
- Schor RH, Steinbacher BC Jr, Yates BJ. Horizontal linear and angular responses of neurons in the medial vestibular nucleus of the decerebrate cat. *J Vestib Res* 1998;8:107–116. [PubMed: 9416596]
- Seidman SH, Bush G, Paige GD, Tomko DL. Perception of translational motion in the absence of non-otolith cues. *Soc Neurosci Abstr* 1998a;24(1):416.
- Seidman SH, Telford L, Paige GD. Tilt perception during dynamic linear acceleration. *Exp Brain Res* 1998b;119:307–314. [PubMed: 9551831]
- Shelhamer M, Robinson DA, Tan HS. Context-specific adaptation of the gain of the vestibulo-ocular reflex in humans. *J Vestib Res* 1992;2:89–96. [PubMed: 1342386]
- Snapp-Childs W, Corbetta D. Learning to walk: individual differences and early strategies. *J Sport Exer Psych* 2005;27 Suppl S:S143–S144.
- Takeda N, Tanaka-Tsuji M, Sawada T, Koizuka I, Kubo T. Clinical investigation of the vestibular cortex. *Acta Otolaryngol Suppl* 1995;520:110–112. [PubMed: 8749094]
- Telford L, Seidman SH, Paige GD. Dynamics of squirrel monkey linear vestibuloocular reflex and interactions with fixation distance. *J Neurophysiol* 1997;78:1775–1790. [PubMed: 9325347]
- Vingerhoets RA, Medendorp WP, Van Gisbergen JA. Time course and magnitude of illusory translation perception during off-vertical axis rotation. *J Neurophysiol* 2006;95:1571–1587. [PubMed: 16319215]
- Wertheim AH, Mesland BS, Bles W. Cognitive suppression of tilt sensations during linear horizontal self-motion in the dark. *Perception* 2001;30:733–741. [PubMed: 11464561]
- Wood SJ, Reschke MF, Sarmiento LA, Clement G. Tilt and translation motion perception during off-vertical axis rotation. *Exp Brain Res* 2007;182:365–377. [PubMed: 17565488]
- Wright WG, DiZio P, Lackner JR. Vertical linear self-motion perception during visual and inertial motion: more than weighted summation of sensory inputs. *J Vestib Res* 2005;15:185–195. [PubMed: 16286700]
- Yong NA, Paige GD, Seidman SH. Multiple sensory cues underlying the perception of translation and path. *J Neurophysiol* 2007;97:1100–1113. [PubMed: 17122319]
- Young, LR. Perception of the body in space: mechanisms. In: Darian-Smith, I., editor. *The nervous system*. Vol. vol III. Bethesda: American Physiological Society; 1984. p. 1023-1066.
- Zupan LH, Merfeld DM. Human ocular torsion and perceived roll responses to linear acceleration. *J Vestib Res* 2005;15:173–183. [PubMed: 16286699]
- Zupan LH, Merfeld DM, Darlot C. Using sensory weighting to model the influence of canal, otolith and visual cues on spatial orientation and eye movements. *Biol Cybern* 2002;86:209–230. [PubMed: 12068787]

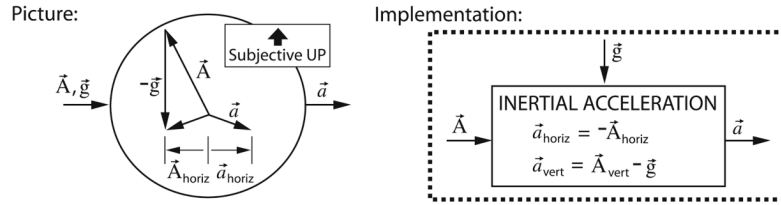
**Fig. 1.**

Off-vertical axis rotation and typical perceptions, shown with a head and simultaneously the polyhedron that represents the head in later figures. **a** Actual motion of rotation about an off-vertical axis. Shown here is clockwise yaw, for which tilt causes the horizontal component of force, and therefore the GIA, to come from the directions, repetitively in order of, back, right, front, and left, **b** typical perception during slow OVAR: a cone-shaped motion. The cone progresses counterclockwise with the GIA due to tilt and centripetal acceleration coming from directions in the same order implied by part (a) of, back, right, front, and left, **c** typical perception during fast OVAR: a cylinder-shaped motion. The cylinder progresses counterclockwise with the GIA associated with centripetal acceleration coming from directions in the same order implied by part (a) of, back, right, front, and left

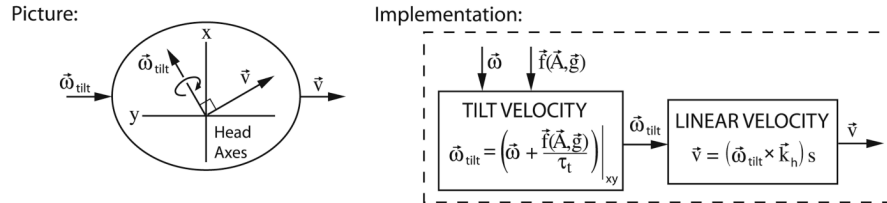
a STANDARD MODEL



b HYPOTHESIS #1: REVERSE TRANSLATION



c HYPOTHESIS #2: PHASE-LINKING OF TRANSLATION TO TILT



d HYPOTHESIS #3: PHASE-LINKING OF TILT TO TRANSLATION

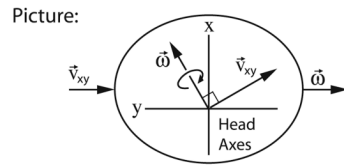


Fig. 2. Models for testing hypotheses. **a** Standard Model. All vectors are in subject coordinates: α = angular acceleration; ω = angular velocity; \vec{i}, \vec{j} = unit vectors giving heading, implemented here as the starting-point earth-horizontal projection of noseward and leftward directions, respectively; \vec{g} = earth-upward vector of magnitude 9.81 m/s²; \vec{A} = gravito-inertial acceleration; \vec{a} = linear acceleration; \vec{v} = linear velocity; \vec{p} = position of an earth-fixed reference point, implemented here as the starting position of the head, to keep track of 3-D position; $\vec{f}(\vec{A}, \vec{g})$ = the vector with magnitude equal to the angle between \vec{A} and \vec{g} , and direction that of rotation from \vec{A} to \vec{g} . The vectors α and \vec{A} are given by the stimulus, and all other vectors are perceptual estimates. Additional intermediate components such as sensor dynamics and internal models

of sensor dynamics are combined into the concise set of time constants shown; for example, semicircular canal dynamics, their internal model, and any extension of the resulting time constant for perception are combined into the single perceptual time constant τ_a . The linear and tilt time constants are τ_l and τ_t , respectively. An internal model of the variables is assumed and necessary, as derivatives depend upon the variables themselves in many of the blocks (explicit loops not shown for these simple dependencies). The model comprises three-dimensional laws of physics except for the circled pieces with time constants, which give tendencies of the perceptual system. The output variables are given from the subject's perspective, in head coordinates, but for scientific purposes of analysis and three-dimensional display in later figures, the output is transformed in the standard way to earth coordinates. *Dashed boxes* indicate pieces replaced by alternative hypotheses as described in parts **(b, c)**, **b** reverse translation model. The earth-vertical component of **a** is calculated in the same way as in the Standard Model, while the earth-horizontal component is reversed from that in the Standard Model. Shown are a graphical representation of the hypothesis and the technical implementation which replaces the *dotted box* in part **(a)**, with vectors defined as in part **(a)**, in addition to $\mathbf{a}_{\text{horiz}}$ and $\mathbf{A}_{\text{horiz}}$ representing the (subjective) earth-horizontal components of **a** and **A**, respectively, **c** model of translation phase-linked to tilt. Linear velocity is linked to the Standard Model's computation of tilt. Tilt velocity, $\boldsymbol{\omega}_{\text{tilt}}$, is defined as the head *xy*-projection of the angular velocity vector including that toward aligning **g** with **A**. Linear velocity is then computed in such a way to be in the same direction as the tilt, e.g., rightward tilt velocity implies rightward linear velocity. Shown are a graphical representation of the hypothesis and the technical implementation using a cross product with a unit vector, \mathbf{k}_h , in the head's *z* direction to give the correct direction of translation, as well as a scaling factor to give the amount of translation relative to the tilt. For this study, $s = 2$ was used; other values simply give different amounts of excursion analogous to inter-individual variation in amount of perceived translation. The technical implementation replaces the *dashed box* in part **(a)**, **d** model of tilt phase-linked to translation. Angular velocity is linked to the Standard Model's computation of head-horizontal linear velocity, represented by \mathbf{v}_{xy} . Shown is a graphical representation of the hypothesis, which is implemented only conceptually as explained in the text

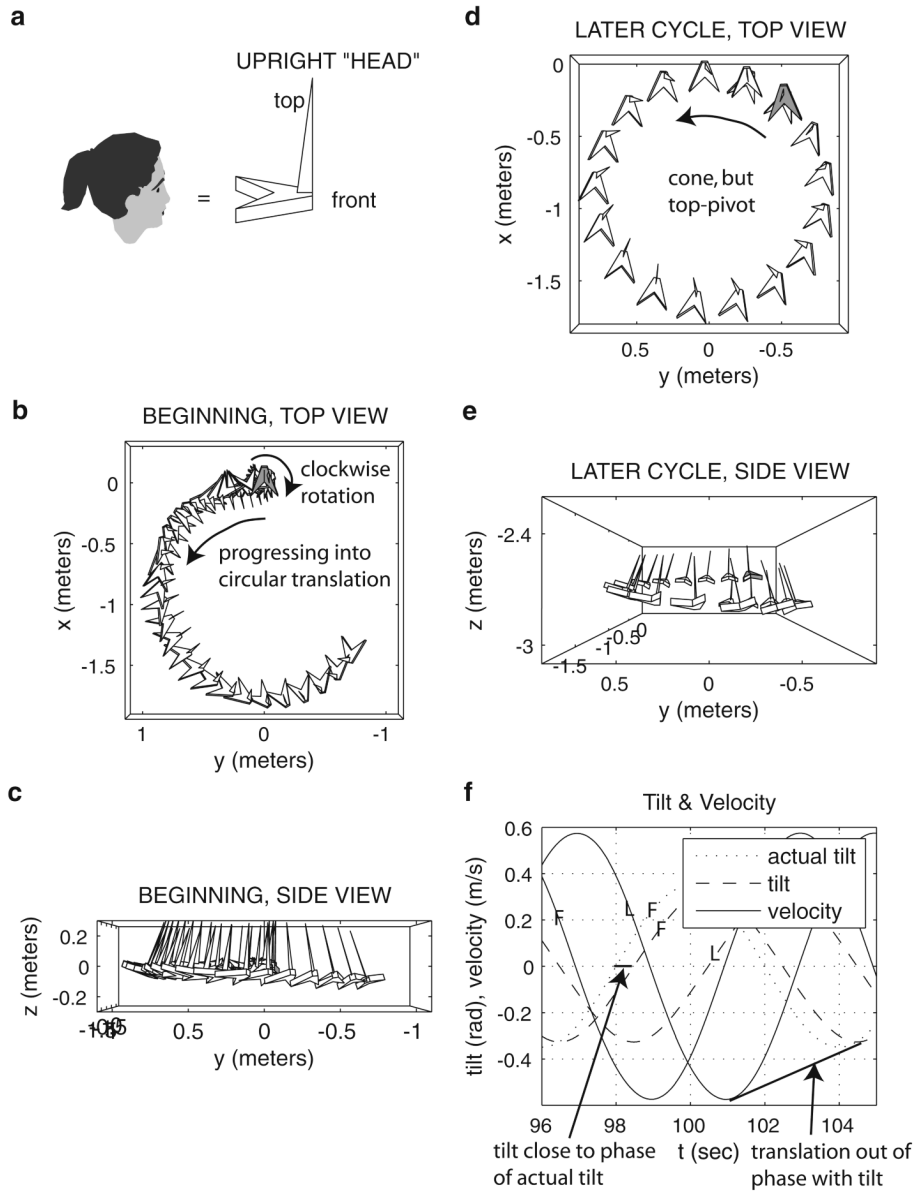


Fig. 3. Standard Model results for slow OVAR, **a** polyhedral “head” used in 3-D animations, for indication of orientations, **b** beginning of Standard Model simulation, *top view*, in freeze-frame format with a polyhedral head showing the location and orientation every 0.5 s (which is 1/16 of an actual rotation). The *gray head* is at time zero, tilted back 20°, and the first jumbled heads are indicating a clockwise rotation, roughly on axis. Translation slowly begins, progresses in a counterclockwise direction. The initial 18 s are shown, during which just over two actual rotations take place, **c** same motion, *side view*, indicating that a slight downward motion begins, **d** later portion of the same Standard Model simulation, starting at the 96 s point and continuing for 9 s, during which just over one actual rotation takes place. The *gray head* is at time 96 s; at that time, the actual head orientation is tilt-back 20°. The motion is progressing in a counterclockwise top-pivot cone, **e** same portion of simulation as in part (**d**), showing continuous downward motion in a side view, **f** tilt and linear velocities during the cycle shown in parts (**d**, **e**). Leftward is indicated by *L* and forward is indicated by *F*. The actual forward

tilt of the subject (i.e., the imposed backward tilt of the GIA) is also shown. Linear velocities are in earth-based coordinates. As reported experimentally by many subjects, the forward tilt has phase close to actual forward tilt. However, the leftward linear velocity, which should be in phase with forward tilt for a bottom-pivot cone, is instead completely out of phase

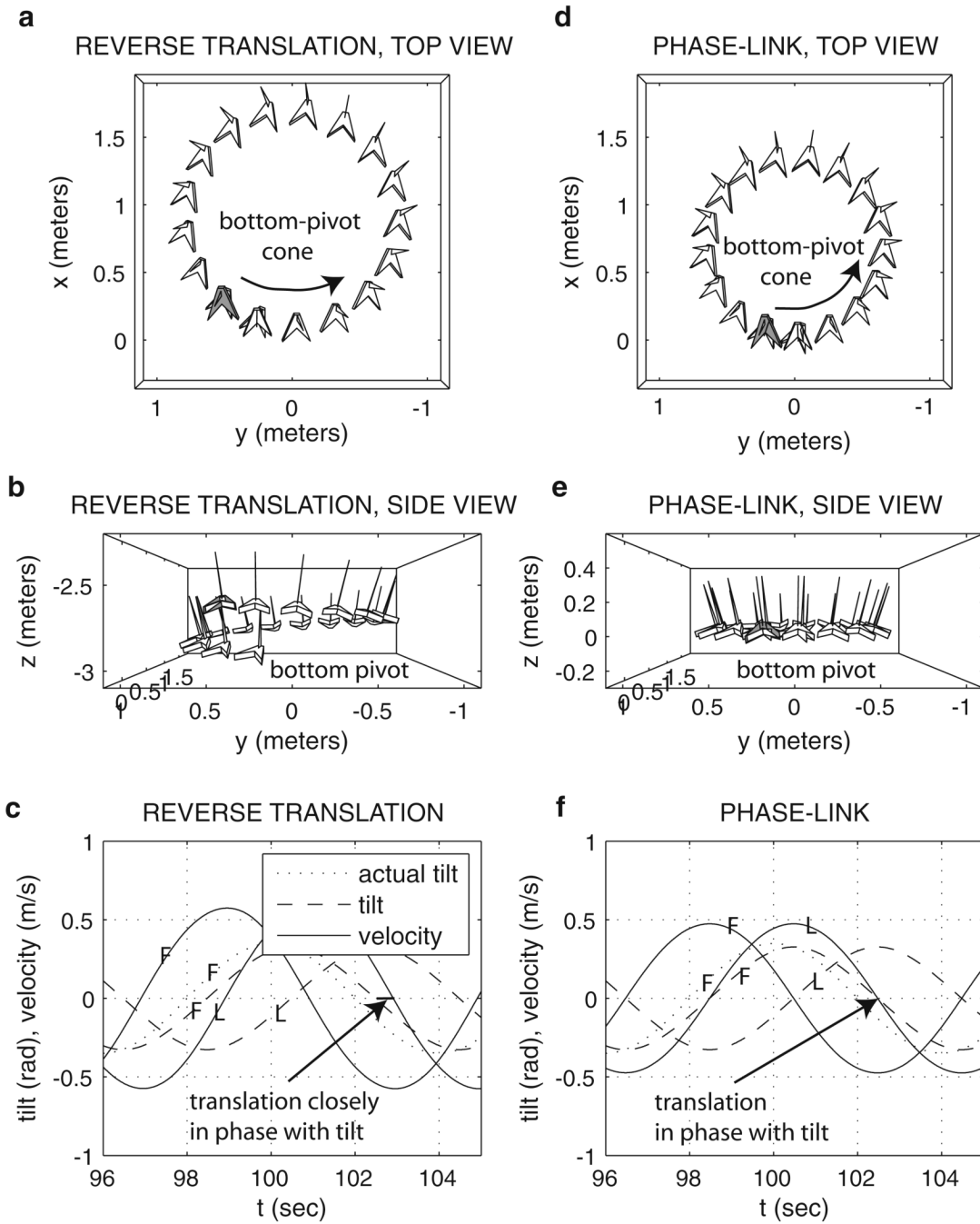


Fig. 4. Results of simulations with alternative Hypotheses #1 and #2, reverse translation and phase-linking to translation to tilt, for slow OVAR, for 9 s starting at the 96 s point. The same conventions are used as in Fig. 3. **a** simulation testing Hypothesis #1 with translation phase reversed. The motion is progressing in a counterclockwise bottom-pivot cone, **b** same motion, side view, showing continuous downward motion, **c** tilt and linear velocities during the cycle shown in parts (**a**, **b**). Leftward is indicated by *L* and forward is indicated by *F*. The actual forward tilt of the subject (i.e., the imposed backward tilt of the GIA) is also shown. Linear velocities are in earth-based coordinates. As reported experimentally by subjects, the leftward linear velocity is closely in phase with forward tilt, **d** simulation testing Hypothesis #2 with

translation phase-linked to tilt. The motion is progressing in a counterclockwise bottom-pivot cone, **e** same motion, side view, **f** tilt and linear velocities during the cycle shown in parts (**d**, **e**), with the same conventions as in part (**c**). As reported experimentally by subjects, the leftward linear velocity is in phase with forward tilt

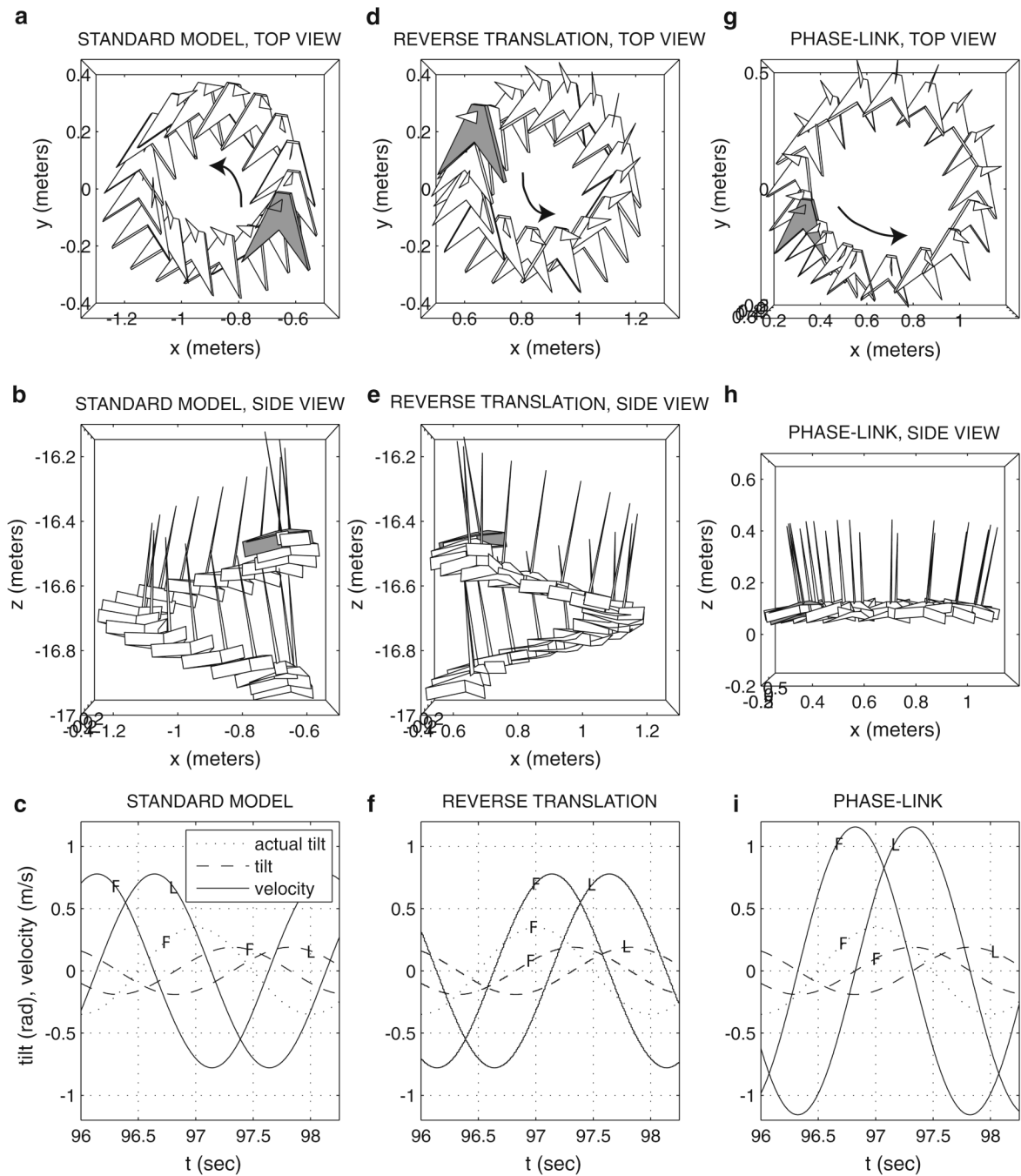


Fig. 5. Fast OVAR, results of simulations with Standard Model and alternative Hypotheses #1 and #2, starting at the 96 s point and continuing for 2.5 s, during which just over one actual rotation takes place. The freeze-frame format has a polyhedral head every 0.125 s (which is 1/16 of an actual rotation). As indicated by the scale, the amount of translation is less than for slow OVAR (Fig. 3, Fig. 4); the figure is therefore zoomed in for a better view. In all 3-D plots, the *gray head* is at time 96 s; at that time, the actual head orientation is tilt-back 20°. **a** Standard Model simulation, *top view*. The motion is circular with the bottom of the head slightly leading the path around the circle, **b** same motion, *side view*, indicating continuous downward motion, **c** tilt and linear velocities during the cycle shown in parts (**a**, **b**). Leftward is indicated by *L* and

forward is indicated by F . The actual forward tilt of the subject (i.e., the imposed backward tilt of the GIA) is also shown. Linear velocities are in earth-based coordinates, **d** simulation with translation phase reversed, *top view*. The motion is circular with the top of the head slightly leading the path around the circle, **e** same motion, side view, showing continuous downward motion, **f** tilt and linear velocities during the cycle shown in parts (**d**, **e**), with the same conventions as in part (**c**), **g** simulation testing Hypothesis #2 with translation phase-linked to tilt. The motion is progressing in a counterclockwise bottom-pivot cone, **h** same motion, side view, **i** tilt and linear velocities during the cycle shown in parts (**g**, **h**), with the same conventions as in part (**c**)

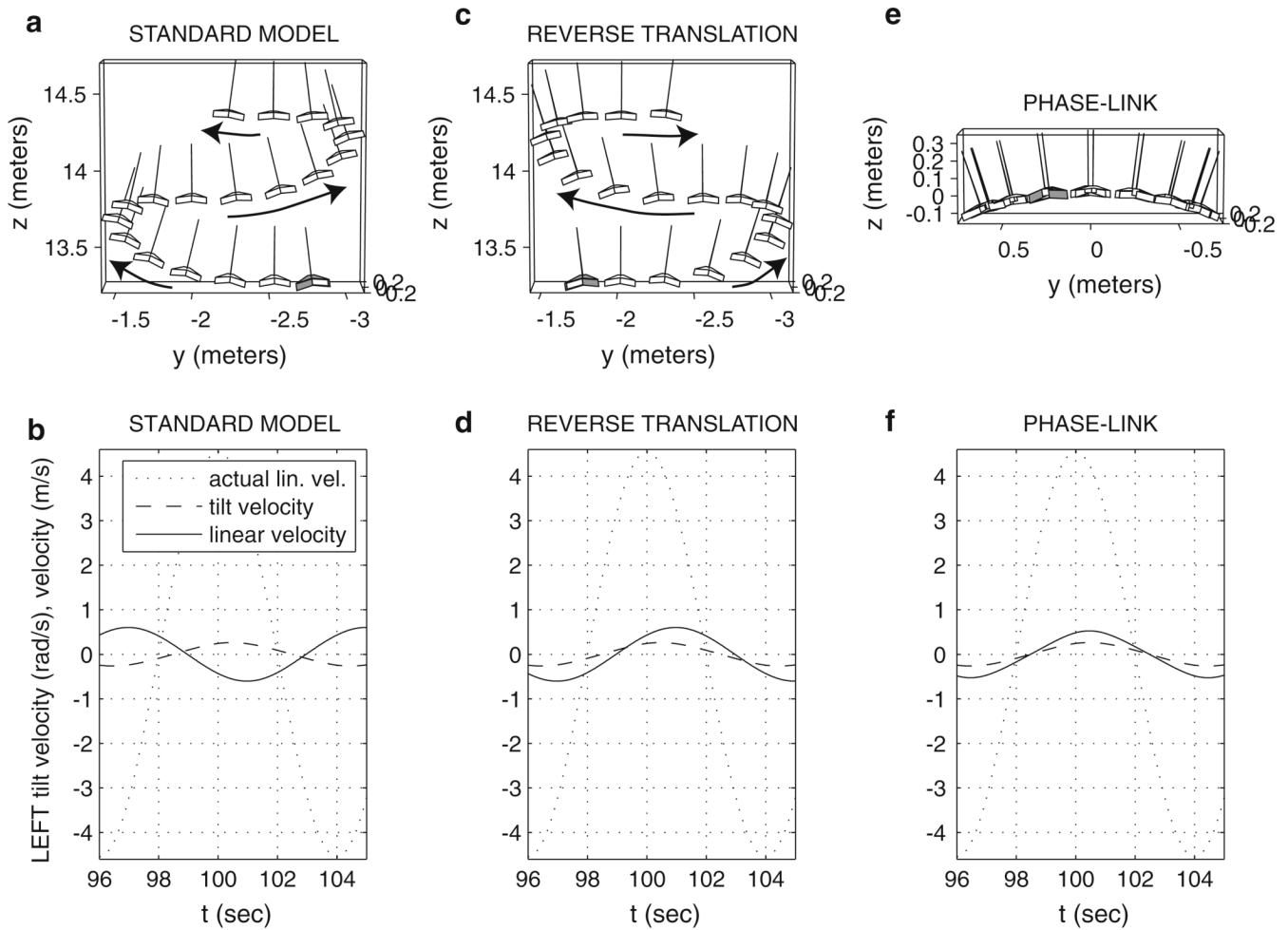


Fig. 6. Horizontal linear oscillation, results of simulations with Standard Model and alternative Hypotheses #1 and #2 for slow ($1/8\text{Hz}$) oscillation, starting at the 96 s point and continuing for 9 s, during which just over one actual cycle takes place. All 3-D plots are shown from the back view, with the “sail” of the head showing the tilt. In all 3-D plots, the *gray head* is at time 96 s; at that time, the actual head position is at center, moving rightward. **a** standard model simulation. The motion snakes upward in a swinging manner, **b** tilt and linear velocities during the motion shown in part (a). The actual linear velocity of the subject is also shown. Linear velocities are in earth-based coordinates, **c** simulation testing Hypothesis #1 with translation phase reversed. The motion snakes upward in a rocking manner, **d** tilt and linear velocities during the motion shown in part (c), with the same conventions as in part (b), **e** simulation testing Hypothesis #2 with translation phase-linked to tilt. The head moves back and forth as over a hilltop, **f** tilt and linear velocities during the motion shown in part (e), with the same conventions as in part (e)

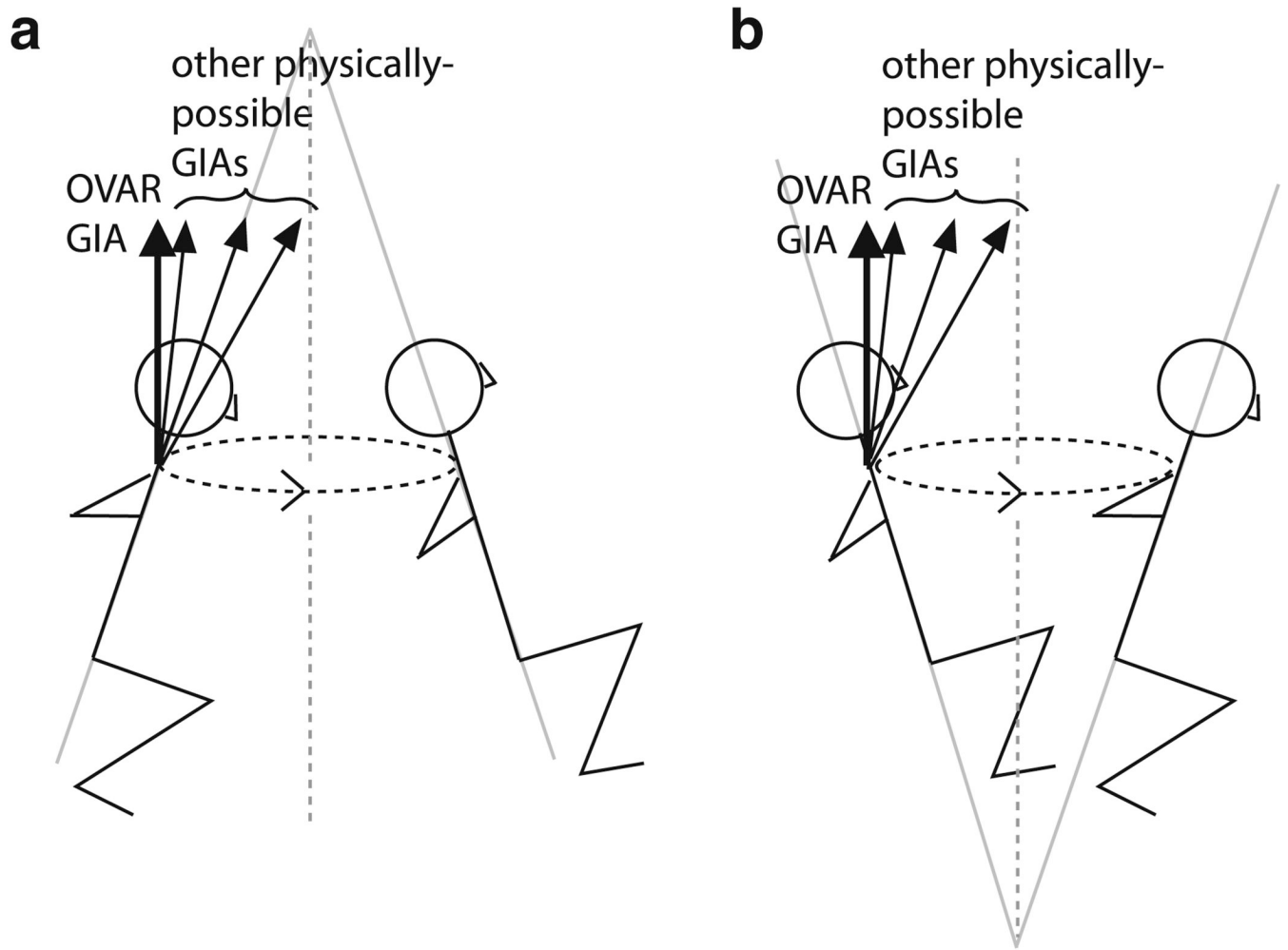


Fig. 7. Two possible perceived cones during OVAR with approximate direction of detected GIA (OVAR GIA with *thick arrow*), as well as other examples of directions of the GIA that would occur during actual conical motion. The other physically possible GIAs point inward toward the axis of rotation because of centripetal acceleration. **a** Top-pivot cone as predicted by the Standard Model, **b** bottom-pivot cone as predicted by phase-linking translation to tilt